https://doi.org/10.5194/egusphere-2025-6333
Preprint. Discussion started: 7 January 2026

Characterizing low and high flow spells and their temporal transitions using baseflow estimates

Guilherme M. Guimarães[1], Maria-Helena Ramos[1], Ilias Pechlivanidis[2]

[1]Université Paris-Saclay, INRAE, HYCAR, Antony, France
[2]Swedish Meteorological and Hydrological Institute, Norrköping, Sweden

Correspondence to: Guilherme M. Guimarães (guilherme.mendoza-guimaraes@inrae.fr)

Abstract. Extreme hydrometeorological events such as floods and droughts cause severe socio-economic and environmental impacts. These impacts can be amplified if hazards occur successively before the system can recover. While the drivers of individual extremes are well understood, the spatial variability and timescales of transitions between high and low flow spells remain understudied, especially regarding their implications for operational management. We propose an analytical framework to detect and characterize these spells using daily streamflow data from 643 catchments in France (CAMELS-FR) over the 1970-2021 period. We use a mixed threshold approach combined with baseflow estimation as an indicator for catchment recovery to identify the spells and analyze their frequency, duration, and temporal transitions. The analysis is carried out at catchment scale and at the scale of French operational flood forecasting centers. We find that short duration high flow spells are predominant across France, while long duration high flow spells are concentrated in northern France. Regarding transitions, they are predominantly consecutive occurrences of the same spell type, with consecutive high flow spells being more common. Our analysis reveals that transitions occurring in less than a month from low to high flows show distinct spatial variability, with the shortest transition durations concentrated in the Rhone-Mediterranean and Rhine-Meuse basins. These short term transitions predominantly occur in autumn and early winter. On the other hand, transitions from high to low flows are typically slow, developing over more than 90 days. These findings highlight the importance of enhancing our knowledge on compound events to better adapt flood disaster and drought management to local contexts and their characteristics.

1. Introduction

The World Meteorological Organization (WMO) reports that floods and storms were the most frequent causes of disasters in Europe between 1970 and 2019, with floods alone being responsible for 38% of the recorded events (WMO, 2021). Moreover, the 2022 European drought has drawn attention to the significant socio-economic costs that can be associated with drought events, as it became the second costliest drought in European history, with estimated $22 billion of total economic losses (AON, 2023), and estimated €3.5 billion insured losses only in France (CCR, 2024). This highlights the need for improved understanding, prediction and management of hydrological variability and extremes.

Risk assessments, which have traditionally focused on single hazard occurrences, are increasingly addressing the interactions among hazards and their transitions in space and time (Leonard et al., 2014; Hillier et al., 2020; van den Hurk et al., 2023). In particular, compound events have been increasingly reported around the world and are usually associated with high social, economic and environmental impacts (De Ruiter et al., 2020; Seneviratne et al., 2021; Ward et al., 2022; Brett et al., 2025). In this context, Zscheischler et al. (2020) proposed a clustering typology that categorizes compound events from a climatic hazard, impact-driven perspective into preconditioned, multivariate, spatially compound, and temporally compound events. The latter refers to a sequence of hazards that occur in a given region, which can cause or intensify an impact as the system has not fully recovered from an event when the next occurs (De Ruiter et al., 2020). Temporally compound events may arise not only from repeated occurrences of the same hazard, such as floods triggered by persistent rainfalls, but also from shifts between contrasting hydrometeorological conditions, such as transitions from drought to floods in the same river basin. Transitions from dry to wet conditions, while often viewed positively for their potential to replenish water resources and restore hydro-

https://doi.org/10.5194/egusphere-2025-6333
Preprint. Discussion started: 7 January 2026

systems, can unexpectedly escalate into catastrophic events under certain physical and social conditions, creating unforeseen challenges for disaster risk managers (Chen and Wang, 2022; Barendrecht et al., 2024; Hammond et al., 2025). For example, Deng et al. (2025) identified that these fast transitions are associated with higher peak discharges and greater economic losses compared to flood events occurring in isolation in Central Europe.

The characterization of hazard transitions has received interest from different perspectives, including, for instance, drought-flood transitions (Li et al., 2016), drought-pluvial seesaws (He and Sheffield, 2020), or wet to warm-and-dry spell transitions (Fang and Lu, 2023). To characterize large-scale and long-term hazards and their transitions, many studies focus on the use of climatological indices, such as the standardized indexes based on precipitation, evaporation or soil moisture (He and Sheffield, 2020; De Luca et al., 2020; Chen and Wang, 2022; Rashid and Wahl, 2022; Chen and Ford, 2023; Qing et al., 2023; Hariharan Sudha et al., 2024). Fewer studies have investigated transitions using streamflow time series, although their use can offer a more direct connection between the dynamics of both drought-to-flood and flood-to-drought transitions and water resources and emergency response management at catchment scale (Li et al., 2016; RahimiMovaghar et al., 2024; Götte and Brunner, 2024; Matanó et al., 2024; Brunner et al., 2025). Research on compound events in hydrology can benefit from using increasingly available large sample sets of long time series of streamflow data to improve methods for hazard detection and characterization, as these datasets are becoming increasingly available (Kratzert et al., 2023). It can also benefit from linking observed occurrences and transitions to catchments' characteristics, physical processes, socio-economic interactions and risk reduction strategies that may influence, or be influenced by, compound events (Ward et al., 2020; Brunner et al., 2021; Barendrecht et al., 2024).

The definition of compound events is usually associated with observed impacts on society and/or ecosystems (Zscheischler et al., 2020). However, when characterizing flood and drought events, local impact databases are often not available, or, when available, do not cover long time periods or extended geographical areas. Efforts have been put into building global impact databases, such as EM-DAT (Delforge et al., 2025), but these have revealed reporting and temporal biases that still have to be assessed for their use in local studies (Jones et al., 2023; Delforge et al., 2025). Additional challenges arise as impact databases often do not sufficiently capture both exposure and vulnerability aspects, leading to discrepancies between hazard detection and recorded impacts (Godet et al., 2025), and reflect an aggregation level that prevents from using them in local studies and time series analyses (Lindersson et al., 2020). To address impacts, hydrologists thus commonly rely on pre-defined thresholds or quantiles to detect high and low flows along a time series of streamflow data (Brunner et al., 2021). The higher (lower) the threshold the more severe and the shorter in duration the high (low) flow event will be, with rare events being usually associated with flood and drought events. Event detection is thus intertwined with event characterization, as variables or thresholds used for detection affect the characteristics of the hazards and their transitions.

Baseflow, primarily determined by the baseflow index (BFI), has been used to characterize hydrological droughts at catchment scale (Van Loon and Laaha, 2015; Hellwig and Stahl, 2018), helping to better understand how meteorological droughts propagate through the physical system (Hellwig et al., 2021), and to examine its connection to dry spell length in well and poorly drained systems (Longobardi and Van Loon, 2018). Moreover, it has been shown that baseflow antecedent conditions strongly influence flood magnitude (Berghuijs and Slater, 2023). Baseflow can also assist in the identification of high flow events, when hydrograph separation techniques are used to isolate the quickflow and the baseflow components from the total streamflow. The separated baseflow can be used to estimate the start and end of an event by applying the condition that the total runoff before and after the peak discharge should equal the baseflow within the event (Mei and Anagnostou, 2015; Tarasova et al., 2018), to identify event end dates only (Fischer et al., 2025; Fischer and Schumann, 2025) or, alternatively, to contribute to the definition of events by considering the non-exceedance of a threshold on the fraction of the baseflow contribution to the total streamflow. To the knowledge of the authors, baseflow separation has not yet been used to detect high and low flow events in a joint framework for compound events.

https://doi.org/10.5194/egusphere-2025-6333
Preprint. Discussion started: 7 January 2026

This study presents an analytical framework for multi-hazard (flood and drought) temporally compound events, which relies on the idea that, in the absence of local impact databases, compound events detection can benefit from focusing on streamflows and the conditions that might be critical for decision-makers from forecasting centers or first responders in the context of disaster risk reduction (e.g. consecutive events without enough time for water levels to be back to normal conditions). The framework considers the detection of high and low flow spells, instead of individual flood and drought events. This allows us to consider also a hazardous situation where, for instance, several high flow events occur consecutively, which can be a risk factor in disaster management. To build this framework, we investigate two research questions related to the detection and characterization of temporally compound events: (1) when we rely only on streamflow time series, how efficient is the framework in detecting hazards using a threshold-based approach combined with baseflow as an indicator for catchment recovery to identify spells of high and low flows? (2) When applied to characterize hazards and their transitions, how can the framework be used to inform decision-makers in risk management and reduction? To address these questions, we apply the framework on 643 gauging stations of the CAMELS-FR dataset in France (Delaigue et al., 2025), using a mixed threshold approach to identify flow spells (Caillouet et al., 2017). Three baseflow methods are evaluated in the assessment. We analyze the spatiotemporal characteristics of consecutive spells and their transitions, both at catchment scale and at the scale of national operational forecasting centers in France. By also focusing on this operational scale, we aim to illustrate the added value of the analysis to local flood forecasting centers.

The manuscript is structured as follows: Section 2 describes the methodology and the dataset on which the analytical framework was applied. Section 3 presents the results for the impact of baseflow separation on spells detection, the characterization of spells at catchment scale, and the assessment of temporally compound events across the country. It is followed by discussions in Section 4 and conclusions in Section 5.

2. Methods and Materials

This paper proposes a methodology in three steps: (i) it first consistently detects both high flow spells (HFS) and low flow spells (LFS) using a mixed threshold approach and baseflow to define the end date of the spells; (ii) it characterizes these spells; and (iii) it analyzes spells transitions. We apply this methodology in a case study in France.

2.1. Spell detection

The threshold-level approach has traditionally been applied to detect hydrological drought events (Van Loon, 2015; Heudorfer and Stahl, 2017; Brunner and Chartier-Rescan, 2024), where an event is defined when streamflows fall below a given threshold. To account for seasonal patterns, the use of variable thresholds, such as seasonal, monthly or daily, has been preferred over using a unique fixed threshold (Brunner et al., 2022; Van Loon and Laaha, 2015). On the other hand, floods are typically detected in a time series by using either a block maxima method or the partial duration series sampling method, which captures values above a threshold (Pan et al., 2022). Although less common, the variable threshold-level approach used for drought identification can also be effectively applied to characterize HFS in a consistent and unified manner (Quesada-Montano et al., 2018). However, in practice, when automatically identifying HFS, its application can result in identifying days above the threshold during the low flow season that actually do not represent high flow conditions in the catchment. Therefore, in this study, we adopt a mixed threshold approach (Caillouet et al., 2017). We select as threshold for a given day the minimum (for LFS) or maximum (for HFS) value between a quantile-based fixed threshold and the monthly threshold associated to that day. This mixed threshold approach is more restrictive for spell detection, while still accounting for some seasonal patterns.

The inclusion of baseflow is another characteristic of the method adopted. When analysing hydrologic floods or drought events, independence between events is often ensured by setting a minimum number of days between occurrences (Diederen et al., 2019; Brunner et al., 2020, 2021; RahimiMovaghar et al., 2024), by using pooling procedures (Hisdal et al., 2024) or by

https://doi.org/10.5194/egusphere-2025-6333
Preprint. Discussion started: 7 January 2026

smoothing the time series with a moving average filter (Fleig et al., 2006). In our study, the focus is on ensuring independence between consecutive spells. While the threshold exceedance can identify the starting date of a spell, we introduce the baseflow as a criterion to determine its end date. The idea is that baseflow can be used as a proxy for determining when the catchment returns to normal conditions, effectively pooling events that may form a spell. We estimated baseflow with three different methods, including the UKIH smoothed minimum method (UKIH, 1980), the Lyne-Hollick (LH) recursive digital filter (Lyne and Hollick, 1979), and the Pelletier-Andréassian (PA) conceptual model (Pelletier and Andréassian, 2020):

- The UKIH method breaks down the streamflow time series into non-overlapping blocks of N-days to identify the minimum daily streamflow of each period and calculate potential turning points, which are then used to estimate the baseflow through linear interpolation. We utilized the lfstat R package (Laaha and Koffler, 2022) with default parameters of five days non-overlapping blocks and turning point factor of 0.9, which were determined by calibration and visual inspection of the estimated baseflow hydrograph from a set of catchments in the UK (Piggott et al., 2005; Hisdal et al., 2024).
- The LH method is based on signal decomposition analysis with one filtering parameter to separate the low frequency baseflow component from the high frequency quickflow component (Duncan, 2019). We applied this method following the guidelines proposed by Ladson et al. (2013), which recommend a filter parameter of 0.925 with 3 passes (forward-backward-forward) for daily data (Ladson, 2013).
- The PA method uses a quadratic reservoir framework implemented in the baseflow R package (Pelletier et al., 2020) to represent the baseflow component as the delayed outflow of a conceptual reservoir. It considers that a fraction of the total streamflow recharges the reservoir, and the outflow is determined by a quadratic function of the reservoir's storage, set to the default value of 1000 mm.

Figure 1 illustrates the spell detection procedure applied to HFS (panel on the left) and LFS (panel on the right). First, the mixed thresholds (Q_t) are calculated: the figure illustrates the threshold based on the exceedance of the 99th percentile (q99) for HFS (blue dotted line) and the threshold based on the non-exceedance of the 20th percentile (q20) for LFS (red dotted line). The start date (t_i) of a HFS (LFS) spell is identified when the streamflow is above (below) the mixed threshold (Q_t). Once the baseflow is calculated (green dashed lines), it helps to define the spell end date. For HFS, we first evaluate the date when the streamflow falls below the threshold and equals (or, depending on the baseflow method used, is close to) the baseflow ($t_{e,b}$). We then search backwards the last date when the streamflow remained above the threshold Q_t, which marks the end of the spell ($t_{e,f}$). For LFS, the date $t_{e,b}$ is defined when the baseflow exceeds the threshold Q_t. The spell end date ($t_{e,f}$) is identified by checking backwards the last date when the streamflow was below the threshold Q_t. To account for instances where streamflow temporarily exceeds the threshold for a few days in low flow condition, an additional step is introduced for LFS detection, which pools together spells if there is only five days or less between them. Finally, the automatic procedure verifies that there is no HFS within the LFS.

https://doi.org/10.5194/egusphere-2025-6333
Preprint. Discussion started: 7 January 2026

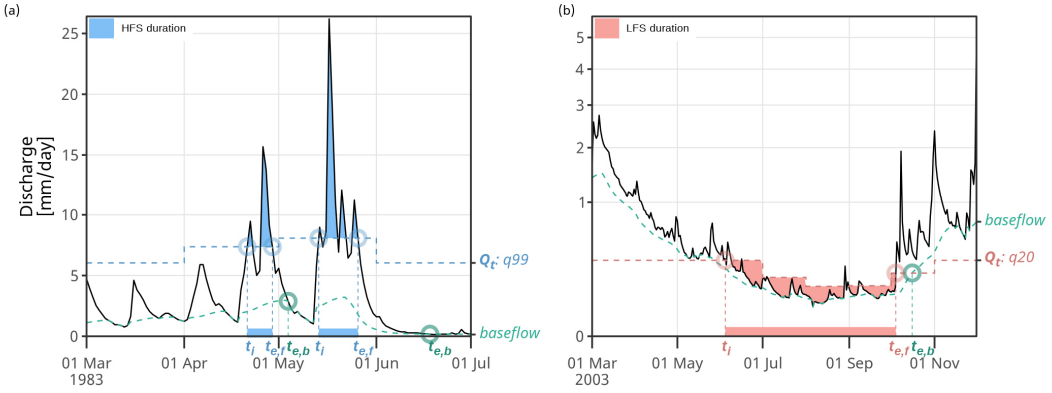

Figure 1 Spell detection procedure for (a) HFS and (b) LFS. Black line shows the streamflow; dashed blue and red lines show the mixed-threshold for HFS and LFS, respectively, considering a 99th percentile (Q_t: q99) and a 20th percentile (Q_t: q20); dashed green line shows the baseflow component using the LH recursive digital filter. Spell start date (t_i), spell end date ($t_{e,f}$), and baseflow end date ($t_{e,b}$) are indicated. In (a) two consecutive HFS are shown with duration of seven and 13 days, respectively, and transition duration of 16 days. In (b) one LFS with total duration of 122 days is shown.

2.2. Spell characterization

We characterize spells with catchment-specific thresholds using two sets of percentiles for the mixed threshold: one more severe, based on the 99th and the 5th percentiles for HFS and LFS, respectively, and one less severe, based on the 95th and the 20th percentiles for HFS and LFS, respectively. To avoid very short LFS that would not be associated with impacts we excluded the LFS with total duration smaller than seven days. For each spell, we calculated the spell duration (difference between start and end dates), the cumulative water deficit (surplus) for LFS (HFS) (in mm) (a measure of severity), the percentage of time the HFS (LFS) spell remained above (below) the threshold, and the number of times the threshold was crossed during the spell duration (which allows us to estimate the number of pooled events within the spell).

For a more robust analysis, we grouped the spells based on their duration, defining the spell categories shown in Table 1. HFS that last up to three days are classified as short duration (HFS_S), between three and 15 days as medium duration (HFS_M), and over 15 days as long duration (HFS_L). For LFS, short duration spells (LFS_S) last between seven and 30 days, medium duration spells (LFS_M) last between 30 and 90 days, and long duration spells (LFS_L) exceed 90 days. Hereafter, we use a generalized notation where *_S, *_M, and *_L refer to short, medium, and long duration spells, respectively, with the asterisk (*) representing either HFS or LFS.

Table 1 Classification of HFS and LFS based on duration and threshold levels. The table summarizes spell categories, including short, medium and long duration events, for high flow and low flow conditions, with associated acronyms and threshold levels used to define the spells.

Spell category		Acronym	Threshold level [percentile]		Spell duration [days]
			More severe	Less severe	
High flow	Short duration	HFS_S	99th	95th	$1 \leq d \leq 3$
	Medium duration	HFS_M			$3 < d \leq 15$
	Long duration	HFS_L			$d > 15$
Low flow	Short duration	LFS_S	5th	20th	$7 \leq d \leq 30$
	Medium duration	LFS_M			$30 < d \leq 90$
	Long duration	LFS_L			$d > 90$

https://doi.org/10.5194/egusphere-2025-6333
Preprint. Discussion started: 7 January 2026

2.3. Spell transitions (temporally compound events)

Four types of spell transitions can be assessed: (i) transition from a low flow spell to a high flow spell (LFS-HFS), (ii) transition from a high flow spell to a low flow spell (HFS-LFS), (iii) transition between two consecutive low flow spells (LFS-LFS), and (iv) transition between two consecutive high flow spells (HFS-HFS). Within each transition type, different spell duration categories (short, medium, long) can also be considered. In our study, only transitions with continuous data are analyzed (i.e., if there are missing data between spells, their transition is not considered in the analysis). Figure 2 illustrates the approach: three short duration high flow spells (HSF_S), one medium duration low flow spell (LSF_M), and one medium duration high flow spell (HFS_M) are detected; three transitions are defined (yellow blocks) for the time span between the first two HSF_S (t1), the third HSF_S and the LFS_M (t2), and the LFS_M and the HFS_M (t3); the transition between the second and the third HFS_S is not considered since streamflow data is missing.

The duration of a transition is quantified in days, measured from the end date of the first spell to the start of the second spell. Our analysis focuses on two categories of interest: transitions with duration less than or equal to 30 days (hereafter, within-a-month) and those with duration between 31 and 90 days (hereafter, seasonal). The within-a-month category includes rapid transitions, with duration less than 14 days, defined by Götte and Brunner (2024). The remaining transitions, those exceeding 90 days, are also quantified but they fall outside the main focus of our study, which emphasizes timescales relevant for short-to-medium term in risk management.

To quantitatively compare the occurrence of transitions across flood forecasting centers (hereafter referred to SPC for "Service de Prévision des Crues" in French), we analyze the frequency of within-a-month and seasonal transitions. For each SPC, we calculate the transition frequency as an exposure-weighted annual rate (i.e., ratio of total transitions and total years of data), so that catchments with longer streamflow data availability contribute proportionally to the regional frequency estimate.

To assess whether a specific region of interest experiences significantly more or fewer transitions than the national average, we calculate the standard score (Z-Score) for each SPC relative to the distribution of frequencies across all SPCs. To account for potential uncertainty in the calculation of the standard score due to the relatively low frequency of these short-to-medium term transitions, we conduct a bootstrap procedure with replacement (10,000 iterations). In each iteration, catchments are resampled, and the standard score is recalculated for each bootstrap sample to generate an empirical distribution of Z-scores. We estimate the 95% confidence interval for each SPC from the bootstrap distribution using the bias-corrected and accelerated bootstrap method, which adjusts for bias and skewness in the bootstrap distribution (Davison and Hinkley, 1997).

To analyze when the transitions mainly occur within the year (i.e. transition seasonality), we evaluate, for each transition, the date corresponding to its midpoint, which is calculated by adding half of the transition total duration to the end date of the first spell. We utilize circular statistics (Ley and Verdebout, 2017) to analyze the transition timing, adapting methodologies established in flood seasonality research (Hall and Blöschl, 2018; Tramblay et al., 2023; Bagheri-Gavkosh and Hosseini, 2023; Fang et al., 2024). Transition dates are converted to angular values to calculate the mean transition date and the concentration index. This index measures the variability of the transition dates around their mean value. To ensure meaningful interpretation of the transition seasonality, we applied the Rayleigh test (Mardia and Jupp, 2000) and the Hermans-Rasson test (Landler et al., 2019), implemented through the sphunif R package (García-Portugués et al., 2024), to test the hypothesis of circular uniformity. Only the streamflow time series for which the null hypothesis of circular uniformity is rejected ($p < 0.05$) are included in the analysis, as circular uniformity would result in mean transition dates that lack statistical relevance or interpretative value.

https://doi.org/10.5194/egusphere-2025-6333
Preprint. Discussion started: 7 January 2026

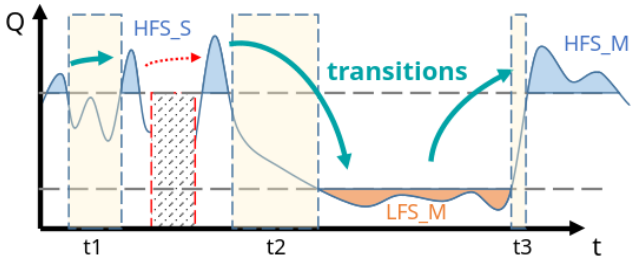

Figure 2 Example of spell transitions illustrating three short duration high flow spells (HSF_S), one medium duration low flow spell (LSF_M), and one medium duration high flow spell (HFS_M), and the transitions (yellow blocks) for the cases where data availability allows their computation (t1, t2 and t3). The dashed red rectangle marks a missing data block, showing the exclusion of the transition between the second and the third HFS_S from the analysis.

2.4. Data and case study in France

We apply our methodology to streamflow data from a set of 643 catchments from the CAMELS-FR dataset in France (Delaigue et al., 2024, 2025), covering a large range of hydroclimatic conditions (from oceanic to continental, mountainous and Mediterranean conditions) (Fig. 3). Catchment mean elevation ranges from a lower quartile of 173 meters above sea level (m.a.s.l.), over a median of 336 m.a.s.l., an upper quartile of 695 m.a.s.l. to a maximum of 2703 m.a.s.l., and catchment areas range from a lower quartile of 98 km^2 over a median of 189 km^2, an upper quartile of 473 km^2 to a maximum of 110,188 km^2. Since the threshold level approach is not suitable for drought identification in intermittent rivers (Van Loon, 2015; Sarremejane et al., 2022), we only considered CAMELS-FR catchments that had less than 5% of days with zero flow. In addition, streamflow data flagged as questionable by the producer for 30 consecutive days or more within the less severe threshold zone, i.e. when streamflow is above the 95th percentile and below the 20th percentile, were removed from the time series. Overall, daily streamflow data are available over the period 1970-2021, with each catchment having at least 25 complete hydrological years, defined as a year with less than 20% missing data. The number of complete hydrological years per catchment ranges from a lower quartile of 37 years, over a median of 45 years, and an upper quartile of 50 years.

To aggregate the results geographically, and illustrate the potential of the temporally compound event analysis to operational hydrology, we rely on the SPCs operated by the French national service (SC Vigicrues), comprising 17 centers at the time of writing, as the spatial units for our regional analysis. For geographical context, these SPCs are presented within six major hydro-administrative regions for hydrological purposes (Fig. 3).

https://doi.org/10.5194/egusphere-2025-6333
Preprint. Discussion started: 7 January 2026

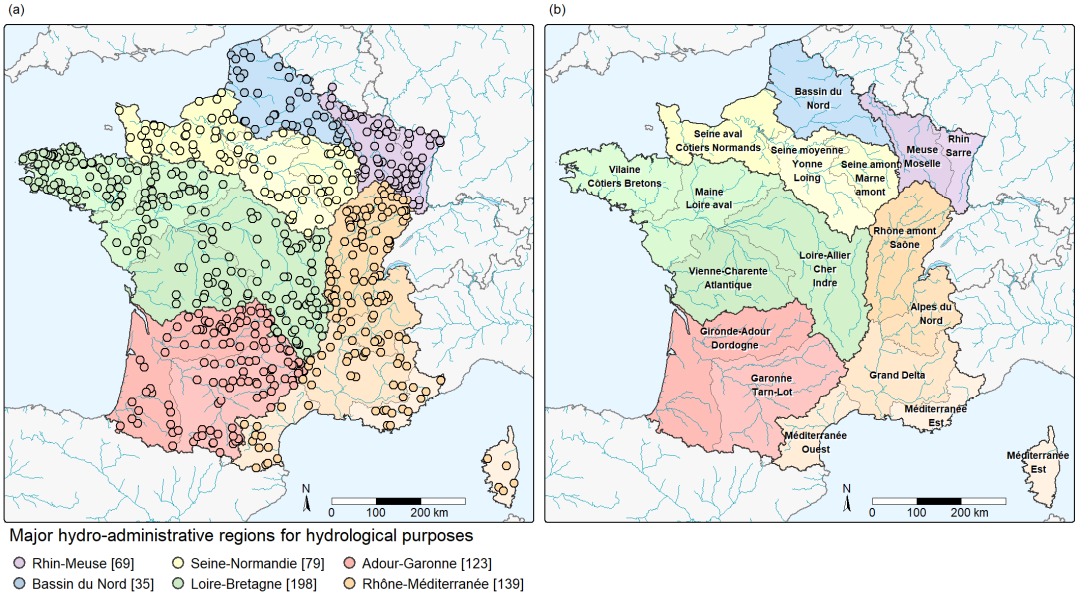

Figure 3 (a) Location of the studied 643 catchment outlets in France, with indication of six major hydro-administrative regions for hydrological purposes (the total number of catchments per region is shown in brackets in the legend), and (b) delineation of the 17 SPCs (river network: Lehner and Grill, 2013; Lehner, 2019; shoreline and political boundaries: Wessel and Smith, 1996; NOAA, 2017; SPC delineation: SC Vigicrues, 2024).

3. Results

3.1. Impact of baseflow separation on spells detection

We first assess the sensitivity of baseflow separation on spell detection, evaluating the impact of the different baseflow methods studied on the number of spells per catchment (Fig. 4), the distribution of spell duration (Fig. 5a), and the percentage of time the spell remained above (below) the threshold for HFS (LFS) (Fig. 5b). Overall, the LH and UKIH methods had similar results in the detection of spells with Pearson correlation coefficients of 0.99 for HFS and 0.92 (less severe threshold) and 0.89 (more severe threshold) for LFS, as shown in Fig. 4. Some differences between these two methods were observed in how baseflow end-date was identified, with UKIH tending to determine them earlier. In some cases, this earlier baseflow end-date identification resulted in the detection of multiple shorter HFS when using the UKIH method, whereas the LH method would detect a single longer spell. Consequently, UKIH identified slightly shorter but more frequent HFS per catchment, particularly when using more severe thresholds, as illustrated by the distribution of spell durations in Fig. 5a. For LFS, the UKIH and LH methods showed opposite behaviors compared to HFS detection. While UKIH detected slightly more HFS per catchment, it was the LH method that detected more LFS per catchment. However, both methods maintained consistent patterns in low flow spell duration and in spell percentage below the threshold (Fig. 5).

https://doi.org/10.5194/egusphere-2025-6333
Preprint. Discussion started: 7 January 2026

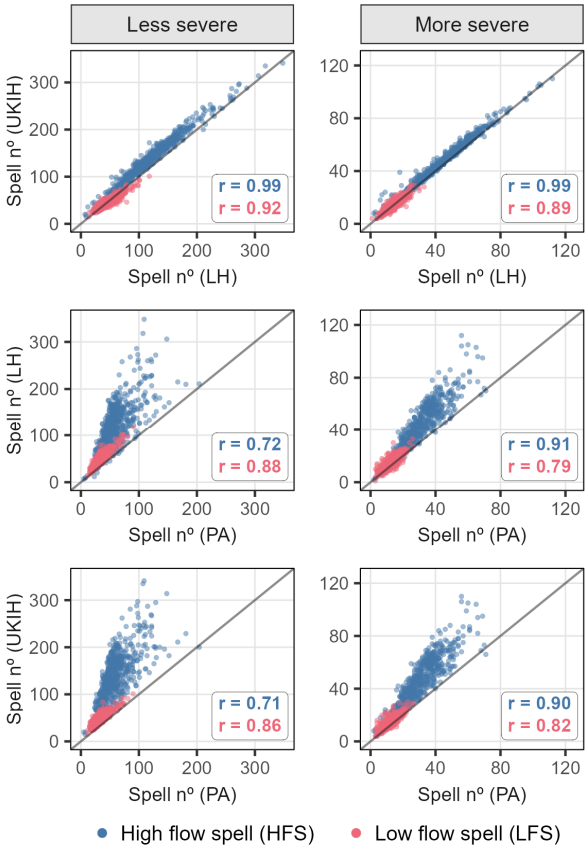

Figure 4 Pairwise comparison of the number of high flow spells (HFS, blue) and low flow spells (LFS, red) per catchment, calculated using three different baseflow estimation methods (LH, UKIH and PA; see text for references) and a set of 643 catchments in France. Spells are detected using both less severe (left panels) and more severe (right panels) thresholds. Each row shows a direct comparison on the number of spells between two methods, as labelled on the x and y axes. The 1:1 line is indicated by the gray line. Pearson correlation coefficients (r) are shown within each panel for HFS (blue) and LFS (red).

The PA method showed a distinct pattern, particularly for HFS detection. The quadratic conceptual reservoir approach in the PA method often did not consistently meet the baseflow end-date condition for HFS, where streamflow contribution should be solely due to baseflow component. Despite implementing a 10% difference tolerance criterion between streamflow and baseflow, the PA method tended to merge multiple HFS into a single prolonged HFS, overestimating HFS duration. This difference is reflected in the lower correlation coefficients when comparing PA with the LH and UKIH methods, especially for the less severe threshold (r = 0.72 and r = 0.71, respectively). The PA method performed better in LFS detection when using the more severe threshold (r = 0.79 and r = 0.82, when correlated with LH and UKIH). Nonetheless, when using less severe thresholds, the PA approach still tended to overestimate the LFS duration, when compared to the LH and UKIH methods (Fig. 5a).

The percentage of time streamflow remained above the threshold during HFS provides additional insight into methodological differences (Fig. 5b). Short duration HFS (1-3 days) have a particular display as they have a bimodal distribution, with one-day and two-day HFS always remaining 100% of the time above the threshold, and three-day HFS either remaining all days above the threshold (at 100% in x-axis in Fig. 5b) or two days above and one day below the threshold (at 66% in x-axis in Fig. 5b). As HFS duration increases (categories medium and long), the percentage of time above threshold decreases across all methods, with the PA method showing consistently lower percentages compared to LH and UKIH. For LFS, Fig. 5b shows short duration LFS still remaining below the threshold for a higher percentage of time compared to medium and long duration

https://doi.org/10.5194/egusphere-2025-6333
Preprint. Discussion started: 7 January 2026

low flow spells. However, unlike HFS, there is not a high difference in the percentage of time the LFS remained below the threshold between medium and long duration spells.

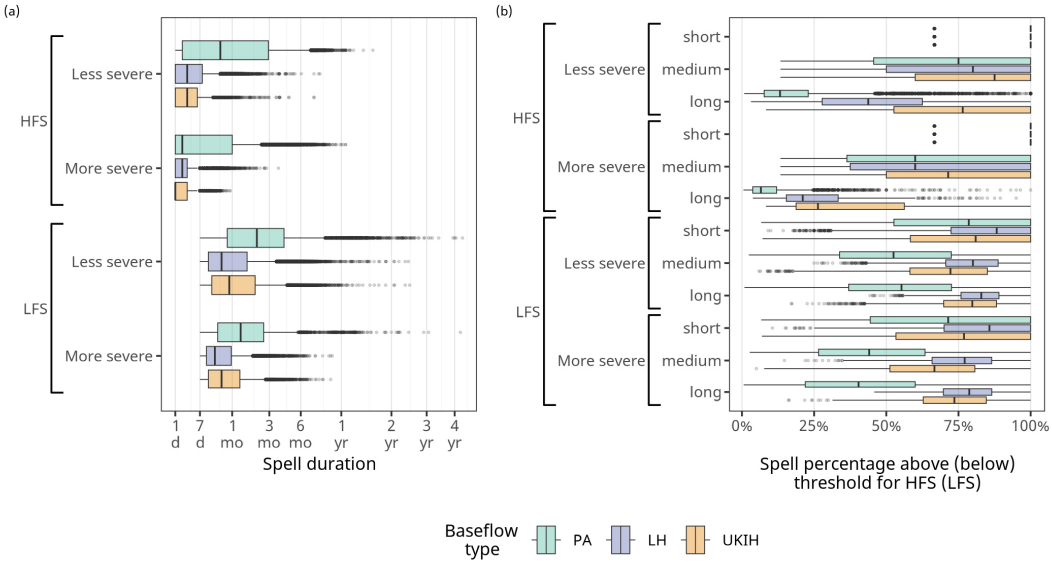

Figure 5 Comparison of baseflow separation methods on hydrological spell characteristics. (a) Boxplot distributions of spell durations for each baseflow separation method (PA, LH and UKIH; see text for references) for high flow spells (HFS) and low flow spells (LFS) for each threshold level. The x-axis is on a non-linear scale to allow the visualization of short-to-medium duration spells (on the scale d represents days, mo represents months, and yr represent years). (b) Boxplot distributions for the percentage of time that the streamflow remains above (for HFS) or below (for LFS) the respective threshold during a spell. These are further categorized by spell duration categories (short, medium and long) as detailed in Table 1.

Figure 6 illustrates the methodological differences between LH and UKIH methods, showing two case studies. The first case is the major 2001 floods in the Somme River basin in northern France, located in the Bassin du Nord hydro-administrative region (Fig. 3a) on the Nièvre River (affluent of the Somme River) (Habets et al., 2010). The second case is the 1996 hydrologic-agricultural drought that hit north and west of France (Barraqué et al., 2010), represented by the Yères River basin, located in the Seine-Normandie hydro-administrative region (Fig. 3a), in the SPC Seine aval-Côtiers Normands (Fig. 3b). In the first case, the LH method detected one continuous long duration HFS while the UKIH method identified 10 separate shorter spells. In the second case, the LH method detected one continuous long duration LFS in 1996, while the UKIH method split this into one LFS_M and one LFS_L, with both methods following with a LFS_L in 1997. This type of fragmentation by the UKIH method may not optimally represent extended HFS, such as those related to groundwater flooding, or LFS that are related to long drought episodes. In both cases illustrated here a single prolonged HFS or LFS better reflects the actual hydrological conditions than multiple shorter events. Given the overall good agreement between UKIH and LH methods across spells metrics (Fig. 5), and the ability of the LH method to better detect spells of long duration, the LH recursive digital filter method will be used for the subsequent analyses in this study.

https://doi.org/10.5194/egusphere-2025-6333
Preprint. Discussion started: 7 January 2026

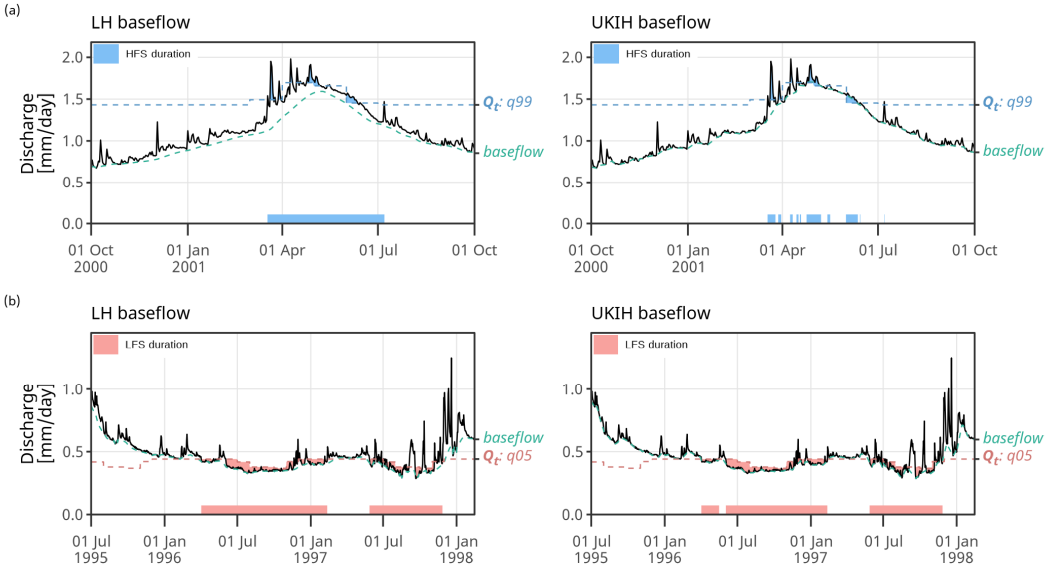

Figure 6 Visualization of spell detection using the LH and UKIH baseflow methods and the more severe thresholds for two cases: (a) the high flow spell (HFS) related to the 2001 flood event in the Somme River basin (Bassin du Nord hydro-administrative region in Fig. 3a), and (b) the low flow spell (LFS) related to the 1996-1997 drought in the Seine-Normandie hydro-administrative region (Fig. 3a), here represented by the Yères River basin located in the SPC Seine aval-Côtiers Normands (Fig. 3b). In each panel, the solid black line is the streamflow, the dashed green line is the baseflow, and the dashed blue (for HFS) or red (for LFS) line represents the more severe threshold. The shaded horizontal bars at the bottom indicate the final detected spells durations.

3.2. Detection and characterization of spells at catchment scale

The use of catchment-specific percentiles allows for the detection of HFS and LFS in each catchment where observed time series of streamflow are available, accounting for regional hydrological variability. Through the application of this methodology to our dataset of 643 catchments in France, we detected 145,721 spells in total across all catchments, with 71.9% classified as HFS and 28.1% as LFS. As anticipated, the majority of spells fell under the less severe threshold category. Within this category, 77,347 HFS were identified, with 54.8% being of short duration, 35.0% of medium duration, and 10.2% of long duration. Similarly, 31,849 LFS were observed in the less severe threshold category, comprising 63.8% of short duration, 24.3% of medium duration, and 11.9% of long duration. On average, each catchment experienced approximately 2.7 HFS per year (first quartile: 2.1 HFS, third quartile: 3.2 HFS), and 1.1 LFS per year (first quartile: 0.95 LFS, third quartile: 1.3 LFS). For the more severe threshold category, 36,525 spells were identified, comprising 27,392 HFS and 9,133 LFS. Within this category, short duration HFS were more common, accounting for 79.2% of all HFS, while long duration HFS constituted only 3.4%. Among LFS, 76.1% were in the short duration category, 19.8% were of medium duration, and 4.1% of long duration. This corresponds to an average of approximately 0.96 HFS per catchment per year (first quartile: 0.68 HFS, third quartile: 1.2 HFS), and 0.32 LFS per catchment per year (first quartile: 0.26 LFS, third quartile: 0.37 LFS). Figure 7 illustrates the spatial distribution of HFS and LFS frequencies across France by spell severity (less severe, more severe), and duration (short, medium, long).

https://doi.org/10.5194/egusphere-2025-6333
Preprint. Discussion started: 7 January 2026

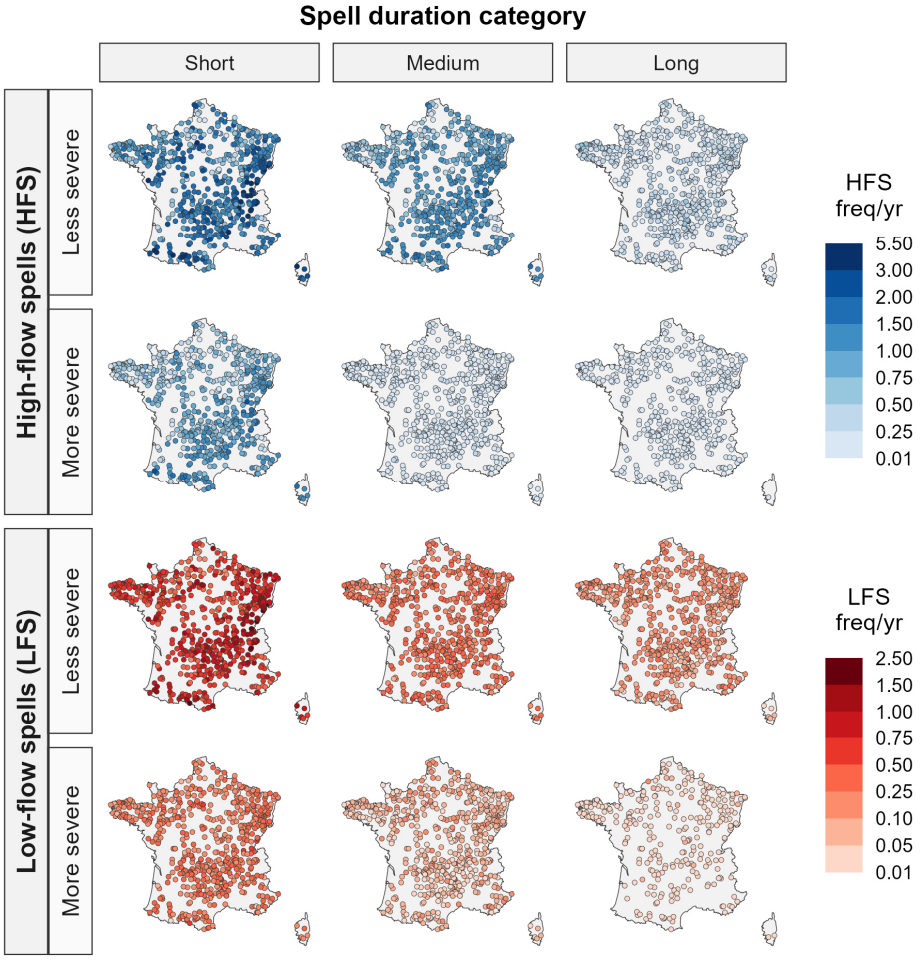

Figure 7 Spatial distribution of the mean frequency per year of spells across 643 catchments in France using the LH baseflow method. The maps are organized by high flow spells (HFS, top two rows, sequential blue scale) and low flow spells (LFS, bottom two rows, sequential red scale). For each spell type is shown the spell severity (rows: less severe, more severe) and duration category (columns: short, medium, and long). Severity and duration categories are defined in Table 1.

The more severe the threshold and the longer the duration, the lower the frequency of spells per year. For the most restrictive case (more severe and long duration), our methodology results in 46% and 73.4% of the catchments with at least one spell for LFS_L and HFS_L, respectively. For all the other cases, there are 95% or more of the catchments with at least one spell. When considering catchments with a minimum of occurrences of five spells, the spatial coverage significantly decreases, especially for the more severe thresholds and long duration spells, with only 3.4% of catchments represented for HFS and no catchment for LFS. This indicates the rarity of extreme and prolonged spells in our case study (catchment dataset and study period).

Interestingly, only two catchments lacked short duration HFS, both located in the Basin du Nord hydro-administrative region (Fig. 3). This region is characterized by slow response catchments sustained by chalk aquifers (Habets et al., 2010). The more severe HFS of longest duration recorded by our methodology, with a total duration of 112 days, was in this region (2001 flood in the Somme River basin, shown in Fig. 6a). Between autumn 2000 and spring 2001, northwestern France experienced exceptional pluvial conditions, leading to flooding of the Somme River and its tributaries, as well as groundwater flooding, where underground water overflowed onto the plateau, particularly in the chalky areas (CCR, 2021). The 2001 flood event in the Somme River basin was notable for its prolonged duration and the extended time required for the hydrologic system to

https://doi.org/10.5194/egusphere-2025-6333
Preprint. Discussion started: 7 January 2026

drain, leading to elevated water levels for at least three months in most areas and up to six months in some regions of the catchment (Pennequin, 2010). In our methodology, multiple individual events occurring in close succession can be pooled into a single spell based on the catchment baseflow condition. The 112-day HFS in the Somme catchment pooled 11 events (Fig. 6a). This was the maximum number of pooled events that resulted from the application of our methodology for HFS. Overall, for HFS across severity and duration categories, the median number of pooled events varied between one to four pooled events.

Figure 8 shows the mean cumulative water surplus (deficit) for HFS (LFS), calculated by summing up the daily discharge (as runoff in mm) that occurred above (below) the threshold during a spell's duration. It is important to recall that, in our spell detection methodology, a spell's total duration does not necessarily mean that the streamflow remains continuously above (for HFS) or below (for LFS) the threshold throughout its entire duration (Fig. 5b). While an increase in spell duration generally corresponds to a higher cumulative surplus (deficit), we observed for HFS that the cumulative water surplus tends to reach a plateau between HFS_M and HFS_L when using the more severe threshold (HFS_M mean: 14.6 mm, first quartile: 3.4 mm, third quartile: 17.1 mm; HFS_L mean: 12.6 mm, first quartile: 3.6 mm, third quartile: 15.4 mm). This counter intuitive result is explained by the proportion of time the spell remains above the threshold for HFS. HFS_M often remains above the threshold for a higher percentage of time compared to HFS_L (Fig. 5b), which may experience more frequent drops below the threshold. Consequently, the cumulative surplus volume does not always increase proportionally with longer durations. On the other hand, the cumulative water deficit, for LFS, reveals a more consistent increase as the duration category extends from short to long duration.

https://doi.org/10.5194/egusphere-2025-6333
Preprint. Discussion started: 7 January 2026

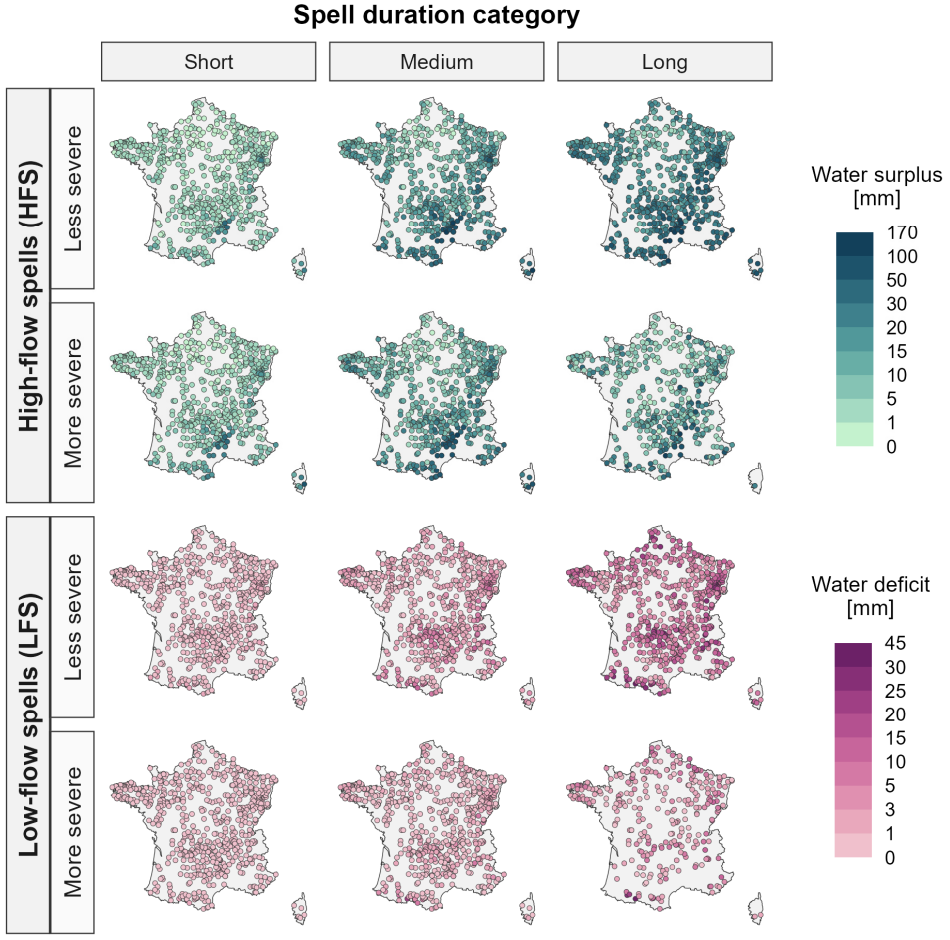

Figure 8 Spatial distribution of the mean cumulative water surplus (deficit) for HFS (LFS) in mm across 643 catchments in France using the LH baseflow method. The maps are organized by high flow spells (HFS, top two rows, sequential green scale) and low flow spells (LFS, bottom two rows, sequential magenta scale). For each spell type is shown the spell severity (rows: less severe, more severe) and duration category (columns: short, medium, and long). Severity and duration categories are defined in Table 1.

As shown in Fig. 5b, long duration LFS remains below the threshold for a high percentage of time, indicating that our methodology effectively captures persistent and sustained periods of low flows. Pooled events were more often observed in LFS detection than in HFS detection, mainly due to typical fluctuations in low streamflow near the threshold. In the more severe threshold and long duration LFS, the median number of pooled events was seven (first quartile: four events, third quartile: nine events), with a maximum of 33 events in the Vonne catchment located in the SPC Vienne-Charente-Atlantique (Fig. 3b) between 19/05/1976 to 02/11/1976. Medium duration LFS had a median of three pooled events (first quartile: two events, third quartile: five events), reaching up to 14 events. In contrast, short duration LFS mostly involved pooling only one or two events, though in one occasion up to eight events were pooled in a station located in the SPC Garonne-Tarn-Lot (Fig. 3b) between 15/11/1985 and 08/12/1985.

Although most identified LFS fell in the short duration category, our methodology effectively captures medium and long duration spells, including those exceeding six months in the more severe threshold and some exceeding one year when using the less severe threshold for spell detection. An illustrative example is the detection of the longest LFS with the more severe threshold in the Seine-Normandie hydro-administrative region (Fig. 3a), shown in Fig. 6b. It lasted 316 days, between 1996 and 1997, and was followed by another LFS_L with 182 days duration in less than four months in the same catchment.

https://doi.org/10.5194/egusphere-2025-6333
Preprint. Discussion started: 7 January 2026

Although this LFS is not related to the most remarkable droughts in 1976 and 2003 in France, it captures the 1996 drought event. This event was characterized by anticyclonic conditions that led to exceptionally low rainfall in winter and spring in the northern regions of France, which propagated to hydrological deficits (CCR, 2018a; Parry et al., 2012), and further depleted soil storages, propagating into agricultural drought in the northern and western regions (Amigues et al., 2006; Barraqué et al., 2010). Even though heavy rainfall during the end of the year partially restored the water levels, deficits persisted into 1997, leading to the reestablishment of drought conditions with precipitation deficits ranging from 25% to over 50% in France (CCR, 2018b). This prolonged LFS detected in our methodology remained below the more severe threshold for 86.7% of its duration, pooling 12 events together.

3.3. Assessment of temporally compound events

We analyzed the frequency and duration of spell transitions (temporally compound events). Transitions can occur between the same or different types of spells (Fig. 2), i.e., from HFS to HFS and from LFS to LFS, but also from HFS to LFS and from LFS to HFS. In addition, one may also consider the different thresholds (more and less severe) and durations (short, medium and long).

Figure 9 shows transition patterns between hydrological spells, allowing us to visualize the proportion of occurrence of each type of transition for three selected configurations. Firstly, we consider only HFS and LFS detected by using the less severe threshold (Fig. 9a). Secondly, only HFS and LFS detected by using the more severe threshold (Fig. 9b). Thirdly, only HFS detected by using the more severe threshold and LFS detected by using the less severe threshold (Fig. 9c).

We can see that consecutive HFS-HFS transitions are the most frequent transition type, accounting for 56% of transitions for the less severe threshold (Fig. 9a) and 63% for the more severe threshold (Fig. 9b). Transitions from HFS to LFS, LFS to HFS, and consecutive LFS were more equally represented, each comprising approximately 15% in the less severe threshold and 12% in the more severe threshold. As mentioned previously, the transition analysis has multiple dimensions. When selecting spells that were detected following a particular threshold of interest, one can obtain different patterns. For instance, the evaluation of transitions using the less severe threshold for LFS threshold and the more severe for HFS (Fig. 9c), the most frequent type of transition is given by consecutive LFS (35% of transitions), followed by consecutive HFS (28%). One can also be interested in examining spell transitions within only some predefined spell duration categories (short, medium and long). Figure 9 shows, for instance, a predominance of transitions between short duration spells (HFS_S and LFS_S). It also shows combinations involving short-to-medium (*_S to *_M), and medium-to-short (*_M to *_S) spells.

https://doi.org/10.5194/egusphere-2025-6333
Preprint. Discussion started: 7 January 2026

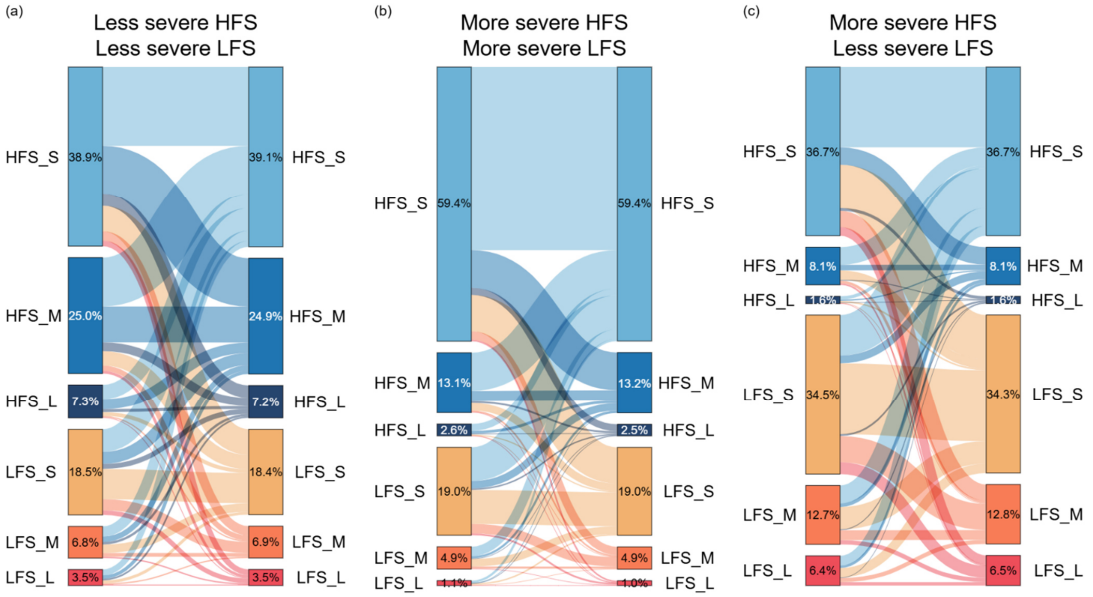

Figure 9 Transition patterns between hydrological spells for three configurations: (a) less severe thresholds for both HFS and LFS, (b) more severe threshold for both, and (c) less severe threshold for LFS with more severe threshold for HFS. Each diagram shows transitions from an initial spell (left column) to a subsequent spell (right column). Spell types are high flow spell (HFS, blue colors), and low flow spell (LFS, orange-red colors), further categorized by duration: short (S), medium (M), and long (L) (see Table 1). The height of each block shows the proportion of that spell type, with percentages on the left representing the proportion of spells starting in each type; while on the right, proportions ending in each type. Darker colour tones represent longer-duration spells, and the colour of each link matches the second (target) spell type. Link widths are proportional to the transition frequency.

While Fig. 9 allows us to focus on the proportion of a particular transition configuration, such as using the less severe threshold for LFS and the more severe threshold for HFS, for instance, it does not inform on the duration of the transitions. Transition durations can vary widely, ranging from as short as 0 day to as long as 5,197 days (approximately 14 years) for the more severe threshold, and up to 2,176 days (about six years) for the less severe threshold. The longest transition durations for both thresholds were recorded in the SPC Bassin du Nord between two LFS for the more severe threshold, and between an HFS and LFS for the less severe threshold. Such long duration transitions can be seen as a catchment with normal flows, or with a long period without experiencing too high or too low flows that could be characterized as HFS or LFS by our methodology. Very short transitions can be seen as an indication of catchments with highly variable flows, going towards extremes in short periods of time. The shortest observed transition duration (0 day) occurred exclusively from LFS to HFS, where a low flow condition abruptly changed to a HFS. In order to investigate this further, we considered the aggregation level offered by the flood forecasting centers in France, as presented in Sect. 2.4. Figure 10 shows the proportions of spell transition duration categories for each SPC, using the less severe threshold for LFS and the more severe threshold for HFS. Transitions are categorized into within-a-month (≤ 30 days, shown in orange) and seasonal (31 to 90 days, yellow), with remaining transitions (> 90 days), in blue. The first two columns in Fig. 10, representing transitions between consecutive spells of the same type (HFS to HFS and LFS to LFS), show relatively homogeneous patterns across the SPCs. The proportion of within-a-month transitions is generally between 17% to 25% of consecutive HFS, and 39% to 47% of consecutive LFS across SPCs. On average, consecutive HFS transitions last 147 days (first quartile: 34 days, third quartile: 219 days), while consecutive LFS transitions last 110 days (first quartile: 16 days, third quartile: 183 days).

Transitions from HFS to LFS (third column in Fig. 10) are relatively slow, with a high proportion of transitions lasting more than 90 days (generally between 77% to 91%). On average, HFS to LFS transitions last 212 days (first quartile: 107 days, third quartile: 242 days), suggesting a gradual development of LFS after an HFS. Within-a-month transitions from HFS to LFS are rare, accounting for only 1.8% of all HFS to LFS transitions, and occurring in only 16% of catchments. The highest proportion

https://doi.org/10.5194/egusphere-2025-6333
Preprint. Discussion started: 7 January 2026

of within-a-month transitions from HFS to LFS (8%) is found in the SPC Seine moyenne-Yonne-Loing, which covers part of the Seine River basin. The SPC Rhône amont-Saône and SPC Alpes du Nord, in the upstream part of the Rhône-Méditerranée hydro-administrative region, were the only regions with at least 25% of HFS to LFS transitions occurring within less than 90 days (the combined within-a-month and seasonal categories).

On the other hand, transitions from LFS to HFS (fourth column in Fig. 10) occur in a shorter time window. The proportion of within-a-month transitions is generally between 10% and 32%, while seasonal transitions are between 27% and 36%. On average, LFS to HFS transitions last 142 days (first quartile: 47 days, third quartile: 157 days). As observed in Fig. 10, there is a more pronounced spatial pattern for this transition type with within-a-month and seasonal transitions predominantly occurring in the Rhône-Méditerranée hydro-administrative region (e.g., SPC Alpes du Nord: 34% within-a-month, 26% seasonal; SPC Méditerranée Est: 37% and 35%, respectively). These shorter transitions are rare in the Loire-Bretagne hydro-administrative region (e.g., only 5% within-a-month occurrence in SPC Vilaine-Côtiers Bretons and 6% in SPC Maine-Loire aval).

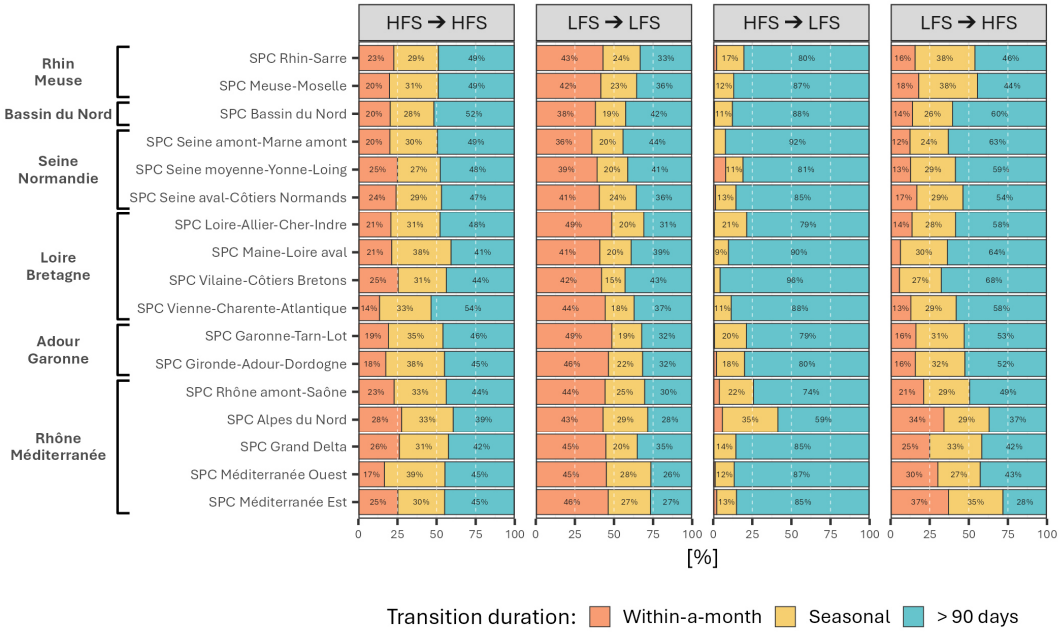

Figure 10 Regional variability in hydrological spell transition durations across 17 SPCs, grouped within France's major hydro-administrative region, using the less severe threshold for LFS and the more severe threshold for HFS. The chart is grouped into four transition types (columns): consecutive HFS, consecutive LFS, HFS to LFS, and LFS to HFS. Each bar shows the proportion of transition durations, categorized as within-a-month transitions (≤ 30 days, orange), and seasonal transitions (31 to 90 days, yellow), and the remaining transitions (> 90 days) are shown in blue.

To better understand the spatial patterns of these short-to-medium-term transitions, Fig. 11 shows the standardized transition frequencies aggregated at the SPC level, using the less severe LFS and more severe HFS threshold. Confidence intervals for these standard scores were obtained from bootstrapping experiments, allowing us to identify SPCs where transition frequencies are above (green) or below (purple) the national mean. The spatial patterns in Fig. 11 indicate regional contrasts. The SPC Alpes du Nord shows transition frequencies above the national mean for all transition types (Z-score above two for either within-a-month or seasonal transitions). On the other hand, SPC Bassin du Nord usually shows lower frequencies in all transition types. Overall, SPCs in the Rhône-Méditerranée, Adour-Garonne, and Rhin-Meuse regions tend to have transition frequencies above the national average, while those in the Bassin du Nord, Seine-Normandie and Loire-Bretagne regions generally have lower transition frequencies.

https://doi.org/10.5194/egusphere-2025-6333
Preprint. Discussion started: 7 January 2026

Specific transition types reveals distinct spatial patterns. For consecutive HFS, northern and western SPCs show less frequent transitions, while SPCs in south of France show higher frequencies. For consecutive LFS, only SPCs in the Rhine-Meuse and Rhône-Méditerranée (Rhône amont-Saône, Alpes du Nord) hydro-administrative regions have transition frequency above average. Regarding HFS to LFS transitions, it is interesting to point out the SPC Seine moyenne-Yonne-Loing for ranking above average for within-a-month transitions but below average for seasonal transitions. The SPC Loire-Allier-Cher-Indre displays the inverse pattern, highlighting regional heterogeneity in transition dynamics within SPCs. For LFS to HFS transitions, SPCs in Seine-Normandie and Loire-Bretagne displays transition frequencies below the national average. On the other hand, all SPCs within the Rhône-Méditerranée hydro-administrative region have within-a-month transitions frequencies above average. For seasonal transitions, SPCs in Rhin-Meuse and Adour-Garonne hydro-administrative regions, and SPCs in Rhône basin exceed the national average.

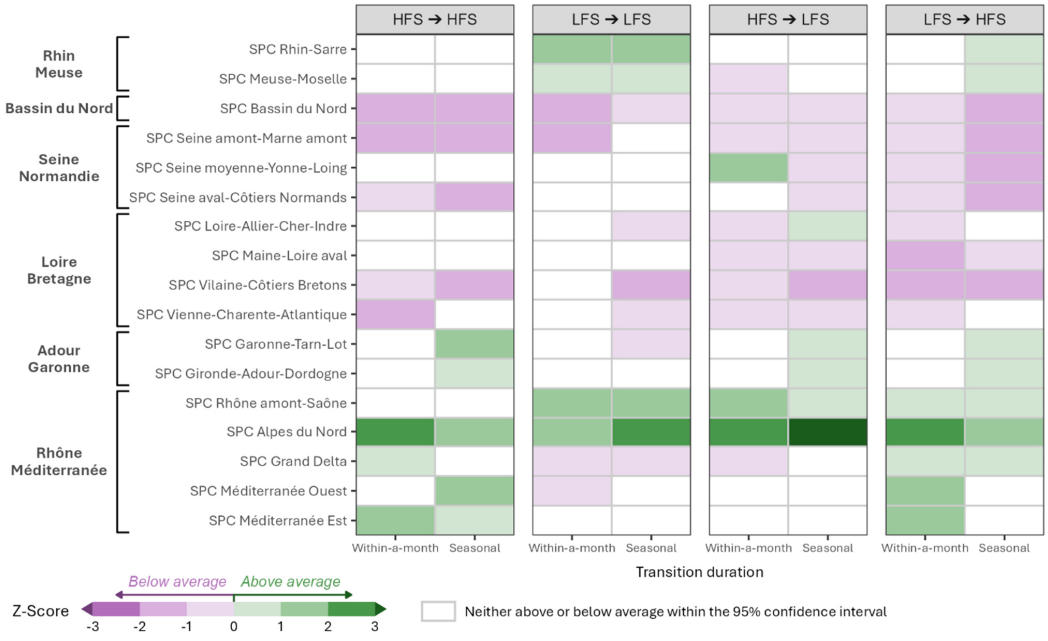

Figure 11 Regional variability in hydrological spell transition frequency across 17 SPCs, grouped within France's major hydro-administrative regions, using the less severe threshold for LFS and the more severe threshold for HFS. The heatmap shows the standard score (Z-score) for each SPC and transition type relative to the national mean. Colored cells indicate SPCs where the transition frequency is above (green) or below (purple) the national mean (i.e., the entire 95% bootstrap confidence interval range excludes zero). White cells represent non-significant results. Columns are divided by transition duration categories in each panel.

Having characterized the proportion of transition categories within each SPC and their frequency relative to the national average, we now explore the specific timescales of short-term transitions. To better analyze spatial patterns for transitions of less than 30 days (within-a-month), Fig. 12 shows maps with the median transition duration aggregated at the SPC level for the less severe LFS and more severe HFS threshold. Four maps are presented, one for each transition type (panels a-d). Each SPC is also represented by a donut chart showing the proportion of transitions between different spell duration categories (e.g., *_S to *_S, *_M to *_S). The first panel shows transitions between HFS; the second, between LFS; the third between HFS and LFS; and the fourth between LFS and HFS. Each map is accompanied by a histogram that shows the distribution of within-a-month median transition duration for all 643 catchments.

For consecutive HFS (Fig. 12a), median values of within-a-month transition duration ranges from 15 days in the SPC Seine amont-Marne amont to 22 days in the SPC Méditerranée Ouest. The donut charts show that transitions involving short duration HFS (HFS_S to HFS_S) are predominant in all SPCs.

https://doi.org/10.5194/egusphere-2025-6333
Preprint. Discussion started: 7 January 2026

For consecutive LFS (Fig. 12b), there is less spatial variability across SPCs, with median transition duration ranging from 14 days to 16 days in the SPC Méditerranée Ouest. These transitions are mainly between short duration LFS (LFS_S to LFS_S), followed by transitions of short-to-medium (LFS_S to LFS_M), and medium-to-short (LFS_M to LFS_S), in a consistent way across all SPCs.

The spatial variability of within-a-month median transition durations between HFS to LFS is shown in Fig. 12c. As identified in the analysis of Fig. 10, these within-a-month transitions are rare (less than 9% across SPCs). Several SPCs (e.g., Méditerranée Ouest, Bassin du Nord, Vienne-Charente-Atlantique) have fewer than four occurrences, with only one occurrence in SPC Grand Delta, and none were observed in any catchments of the SPC Seine amont-Marne amont. Despite the low transition count, some SPCs show short within-a-month median transition duration, such as 10 days in SPC Méditerranée Est. For the SPCs where these transitions occur, the donut charts show they are predominantly from short-duration HFS (HFS_S to LFS_*). The rapid transitions occurring between HFS to LFS, are mainly preceded by a LFS in the previous two weeks (70% of rapid transitions between HFS to LFS). For example, a tributary of the Adour River (in SPC Gironde-Adour-Dordogne), recorded in 2003 a medium duration LFS that was interrupted by a HFS, which then transitioned back to LFS in 10 days. Other examples similar to this were found across all six major administrative regions for hydrological purposes.

The spatial variability for transitions from LFS to HFS within-a-month (Fig. 12d) is characterized by shorter transition durations in the Mediterranean SPC regions, with a median transition duration as short as eight days in the SPC Méditerranée Est (Corsica included) and in the SPC Méditerranée Ouest, followed by SPC Grand Delta (12 days) and SPC Alpes du Nord (13 days). Rapid transitions, occurring within two weeks, were also observed in the Rhin-Meuse hydro-administrative region (SPC Rhin-Sarre and SPC Meuse-Moselle, with median values of 12 days and 13 days, respectively). The SPCs with the highest median transition durations are concentrated in the Loire-Bretagne and Seine-Normandie regions, with median values between 17 days and 22 days. In this group of the transitions, we mostly encounter transitions to short duration HFS (LFS_* to HFS_S, light grey, rose and red colors in the donut charts), and, to a lesser extent, to medium duration HFS (LFS_* to HFS_M). Transitions to long duration HFS (LFS_* to HFS_L) are more observed in the Seine-Normandie hydro-administrative region.

https://doi.org/10.5194/egusphere-2025-6333
Preprint. Discussion started: 7 January 2026

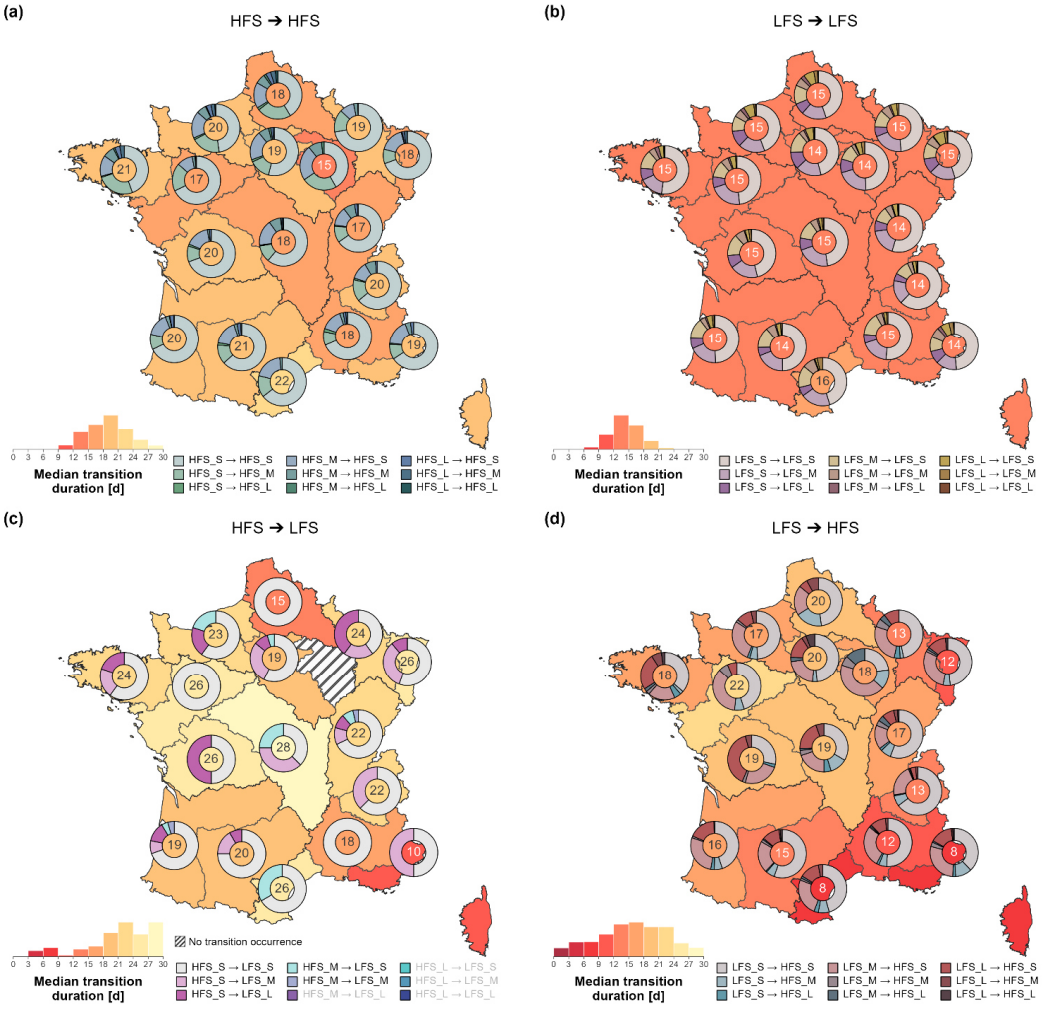

Figure 12 Regional variability of median transition duration of within-a-month spell transitions, aggregated at the SPC level (SC Vigicrues, 2024). All panels use the less severe LFS and more severe HFS threshold combination. The panels show all the four possible transition types: (a) HFS to HFS, (b) LFS to LFS, (c) HFS to LFS, and (d) LFS to HFS. Dark red colours indicate shorter transition duration while yellow light colours indicate longer transition duration. The donut charts show the proportion of transitions between spell duration categories (e.g., *_S to *_S, *_S to *_M, see Table 1). The number in the center of each donut is the median transition duration (in days) for that specific SPC. The histograms at the bottom of each panel indicate the distribution of within-a-month median transition duration for all 643 catchments for that transition type.

Transitions can occur in different times of the year. To investigate their seasonality across space, we evaluated the midpoint date of each transition and analyzed its timing using circular statistics. Figure 13 presents the mean transition date for within-a-month transitions, using the less severe LFS and more severe HFS threshold combination. Figure 13 is divided into four panels, one for each transition type, and in each panel, the color indicates the mean transition timing (month), and the circle size represents the concentration index, with a larger circle indicating a more consistent seasonality (e.g., concentration index of one means that all transitions occurred in the same Julian day of the year). The mean seasonality month is only indicated for stations that reject the circular uniformity tests hypothesis (p-value <0.05) and have at least two transitions.

When considering within-a-month spells transitions, we observe that consecutive HFS transitions (Fig. 13a) predominantly occur during winter months (December to March). Among the catchments showing significant seasonality for this transition, approximately 90% show this winter timing, mainly concentrated in northern and western France. These transitions show moderate to high concentration indices, with an average of 0.83 (minimum: 0.46, first quartile: 0.75, third quartile: 0.94). On

https://doi.org/10.5194/egusphere-2025-6333
Preprint. Discussion started: 7 January 2026

the other hand, consecutive LFS transitions (Fig. 13b) mainly occur in the summer (July to September) across all French territory, and also show moderate to high concentration indices, with an average of 0.74 (minimum: 0.43, first quartile: 0.67, third quartile: 0.83).

For within-a-month transitions from HFS to LFS (Fig. 13c), the seasonality is mainly statistically insignificant, with only two stations showing a significant mean seasonality, one in May (in SPC Gironde-Adour-Dordogne), and one in June (in SPC Seine moyenne-Yonne-Loing).

Finally, transitions between LFS to HFS (Fig. 13d) occur primarily in the autumn and early winter (October to December), particularly in the Mediterranean and Rhin-Meuse regions. These transitions show moderate to high concentration indices, with an average of 0.86 (minimum: 0.56, first quartile: 0.8, third quartile: 0.96), indicating a well-defined seasonality pattern.

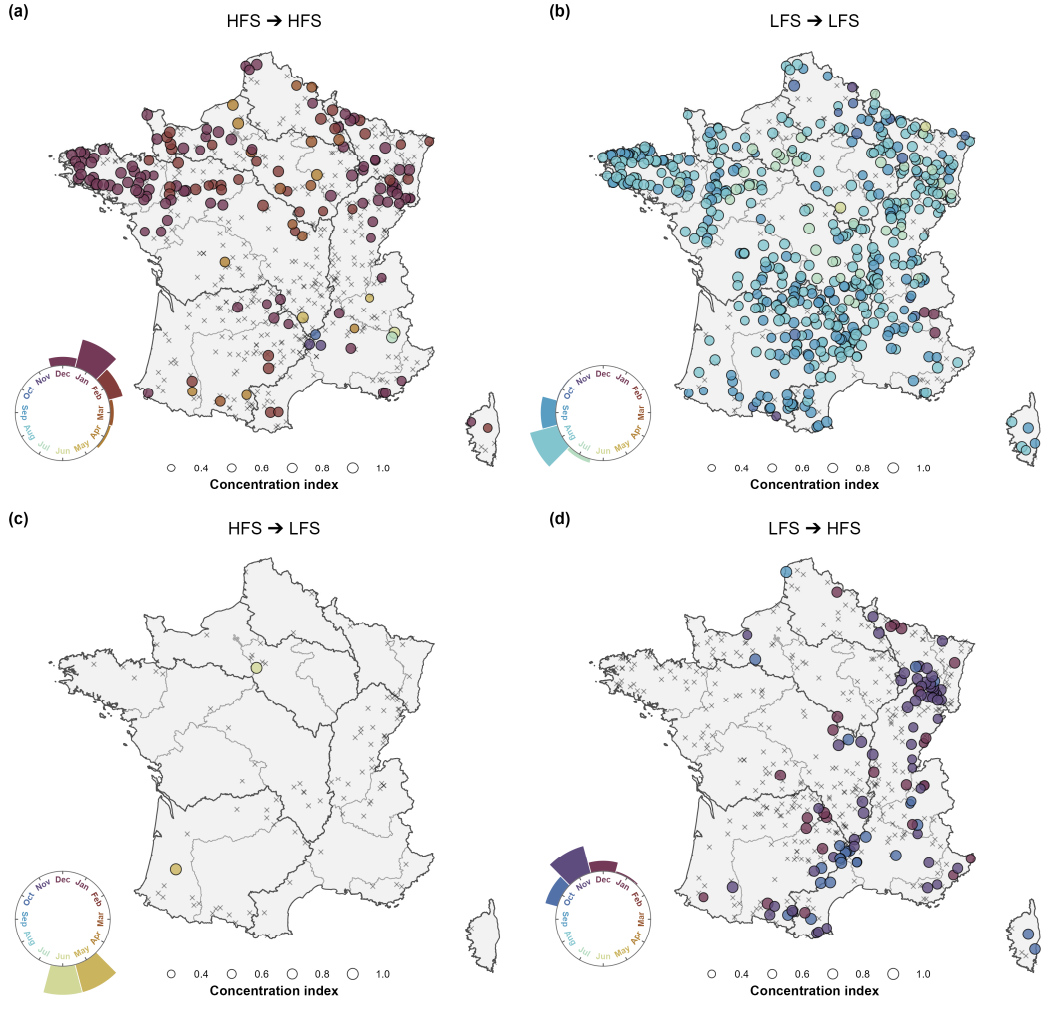

Figure 13 Mean seasonality of within-a-month spell transition across 643 catchments. All panels use the less severe LFS and more severe HFS threshold combination. The panels show all the four possible transition types: (a) HFS to HFS, (b) LFS to LFS, (c) HFS to LFS, and (d) LFS to HFS. The size of the circle represents the concentration index, and the colour indicates the mean timing of these transitions, while the circular barplot shows the proportion of mean transition in each month. Catchments with detected transitions but no significant mean seasonality at p-value of 0.05 are marked in grey x. (SPC delineation: SC Vigicrues, 2024).

https://doi.org/10.5194/egusphere-2025-6333
Preprint. Discussion started: 7 January 2026

4. Discussion

4.1. Integrating baseflow estimates into spell detection

Our approach for detecting high flow spells (HFS) and low flow spells (LFS) for hydrological compound event analysis relies on daily streamflow data only. It is characterized by the integration of a mixed monthly threshold method to separate high and low flows in the times series, and a baseflow estimation method to bring together events that form unique spells.

The use of a mixed monthly threshold method allowed a more robust detection of spells. For HFS, it allowed the detection of spells that deviate from normal seasonal patterns during high flow periods, or of spells that were intense enough during low flow periods to surpass the fixed annual threshold. For LFS, it detected spells deviating from normal seasonal patterns, primarily during the low flow period, consistent with the method proposed by Caillouet et al. (2017). It must be noted that, while the monthly thresholds effectively captured seasonal variability, they can occasionally introduce artificial "staircase patterns" (Heudorfer and Stahl, 2017) when transitioning from one month to another. This can potentially affect the continuity of the detected spells, with abrupt terminations of spells, and a possible solution could be implementing a smoothed daily threshold to further enhance the representation of spell end points.

In our approach, spell end points were defined with the help of baseflow estimations. From the comparison of three different methods, we suggest adopting the LH recursive digital filter (Lyne and Hollick, 1979), which demonstrated superior performance, particularly in capturing long duration high flow spells as a single continuous spell. This can be crucial for detecting groundwater flooding events without fragmenting the same event into several smaller spells. Other studies have shown that groundwater flooding is often overlooked in traditional flood inundation modeling (Collins et al., 2020), despite its distinct impact characteristics, often causing severe economic losses due to durations extending from weeks to several months (Kreibich and Thieken, 2008). Our methodology, allow us to consider groundwater influences through the baseflow estimation, with impact on preventing spell fragmentation. By capturing the full extent of these long duration spells, we can better identify threats through a mechanism similar to preconditioned compound events (Zscheischler et al., 2020). In these situations, even a moderate rainfall occurring during an ongoing spell can rapidly develop into a hazardous condition, as the catchment has not yet recovered to normal baseflow conditions. This mechanism is supported by Berghuijs and Slater (2023), who found that antecedent baseflow conditions often have a stronger and longer lasting influence on flood magnitude than either antecedent soil moisture and short-term extreme precipitation. The importance of baseflow in determining catchment response is further reinforced by Brunner et al. (2025), who demonstrated that, across European catchments, high baseflow indices and storage properties were found to dampen the propagation of meteorological dry to wet transitions to hydrological ones, preventing rapid transitions from dry to wet states.

4.2. Characterization of hydrological spells

We classified spells into short, medium, and long duration categories to facilitate their characterization and analysis. As noted by Götte and Brunner (2024), there is currently no consensus on how to define or characterize transitions between hydrological extremes, and, by extension, how to categorize spell durations. Our duration thresholds of 3 and 15 days for HFS and 30 and 90 days for LFS were selected after preliminary analyses. We aimed to balance statistical robustness and hydrological relevance, providing comprehensive catchment representation in all categories. While the selection of specific duration thresholds is inherently subjective, our categorization allowed us to effectively capture the range of event durations observed across French catchments and provided a framework for analyzing transition dynamics.

As expected, long duration spells of extreme events are rare cases in our analysis. Using the 99th percentile threshold, long duration HFS (above 15 days duration) were observed in less than half of the studied catchments. In catchments where they occur, these spells are rare, occurring on average only once every 20 years in the most affected catchments. The spatial distribution of HFS with longest durations shows a concentration in northern France, consistently with regions characterized

https://doi.org/10.5194/egusphere-2025-6333
Preprint. Discussion started: 7 January 2026

by chalk aquifer dynamics and by catchments with long memory (de Lavenne et al., 2022). In aquifer dominated systems, groundwater contributions can sustain elevated streamflow conditions over extended periods, eventually generating groundwater flooding, as mentioned previously.

Beyond detection, spell characterization can also provide insights for risk managers. In our study, it was shown that long duration HFS are not necessarily the most severe in terms of accumulated water volume. It was observed that streamflow in long duration HFS tends to remain above the threshold for a smaller percentage of time compared to medium duration HFS. This is particularly observed when using the higher thresholds (99^{th} percentile compared to 95^{th}), where even short duration HFS can occasionally exhibit higher accumulated water surplus than long duration HFS (Fig. 8). This was illustrated in the Mediterranean area (Rhône-Méditerranée hydro-administrative region, Fig. 3), where approximately 19% of short and medium duration HFS had greater accumulated water surplus than the maximum observed in long duration HFS within the same catchment.

4.3. Added value of the approach to understand spatial patterns of hydrological transitions

The classification of spell duration categories allows the identification of potentially more severe consequences in temporally compound settings, such as successive long duration spells or transitions from long duration LFS to medium or long duration HFS. These combinations are potentially more impactful than transitions between shorter duration spells. The analysis of transition between hydrological spells can reveal important patterns and enhance knowledge on compound events. In our study, we observed that transitions predominantly occur between short duration spells and within the same type of spells, either consecutive HFS or LFS in France. For example, within-a-month transitions between two short duration spells are more common than transitions from long duration LFS to short duration HFS, and transitions between two long duration spells are rarer. This frequency distribution reflects not only the prevalence of shorter hydrological spells, but also highlights the statistical challenge of analyzing rare, potentially high impact transitions between prolonged extreme conditions (Brunner et al., 2021).

We also investigated transitions from HFS to LFS. According to Hammond et al. (2025), sub-seasonal flood-to-drought transitions involve mechanisms that quickly deplete or fail to replenish surface and subsurface storage, such as early snowmelt, rain-on-snow events, or intense precipitation leading to high runoff partitioning. In our study, we identified that HFS to LFS transitions are predominantly slow, with the majority lasting over 90 days, while sub-seasonal within-a-month transitions are rare. However, for the rare cases where these rapid transitions did occur (in less than 14 days), our analysis indicates they were usually linked to antecedent low flow conditions in the previous two weeks, often acting as brief interruptions of a persistent LFS. This dynamic was detected in the 2003 drought, for instance, in a tributary of the Adour basin (see Fig. 3). Following a summer characterized by record high temperatures and an absence of precipitation leading to drought conditions in France, the region experienced two rapid transitions: from LFS to HFS, and returned back to LFS. The brief HFS interruption corresponds to intense precipitation events recorded in September 2003 (DIREN Midi-Pyrénées, 2003). These events likely generated high runoff partitioning that prevented significant recharge, causing the catchment to quickly revert to low flow conditions.

Moreover, we identified distinct patterns for the mean seasonality across different transition types. Within-a-month transitions showed a lower proportion of significant mean seasonality when compared to seasonal transitions, especially for consecutive HFS and transitions from LFS to HFS and HFS to LFS. Within-a-month and seasonal transitions from LFS to HFS predominantly occurred between October and December across most of France, with only a few high elevation catchments showing a preferential mean seasonality between February and May, mainly for seasonal transitions, located in the Alps and Pyrenees. This timing aligns with the broader European patterns identified by Brunner et al. (2025), who found that hydrological transitions from drought to floods generally occur in winter and spring across most of Europe, except in the Alps and Scandinavia where they tend to happen in summer. Consequently, the October-December predominance of within-a-month

https://doi.org/10.5194/egusphere-2025-6333
Preprint. Discussion started: 7 January 2026

LFS to HFS transitions in our study likely reflects the typical French hydrological regimes with autumn/winter precipitation following the summer low flow periods. This timing differs slightly from the findings of Götte and Brunner (2024) in the Contiguous United States, where low elevation catchments showed a variable timing, although they similarly identified that transitions in high elevation, snowmelt-driven catchments tend to occur in summer.

Insights into spatial patterns can also be gained from the analysis of transition characteristics. In France, Mediterranean catchments showed very short LFS to HFS within-a-month transition durations, with median transitions of just eight days in the SPC Méditerranée Est (including Corsica) and SPC Méditerranée Ouest. Similar rapid transitions were observed in the SPC Grand Delta and SPC Alpes du Nord within the Rhône-Mediterranean hydro-administrative region, as well as in the Rhin-Meuse hydro-administrative region (SPC Rhin-Sarre and SPC Meuse-Moselle). These regional differences may be linked to distinct precipitation regimes, with Mediterranean regions experiencing more intense convective rainfall events with flashy behavior that can promptly terminate the low flow conditions (Vigoureux et al., 2024).

5. Conclusions

In this study, we propose a method to detect hydrological spells of high and low flows from streamflow data, consisting of a mixed threshold-based approach combined with a baseflow estimation technique. The method was developed with the goal of characterizing spells in a joint framework that could be consistently applied to both high flows and low flows. We illustrated the method using streamflow data from a large sample of 643 catchments in France, with daily data available for 25 to 51 complete years, depending on the catchment. The results obtained from the development and application of the method highlighted the following:

- Instead of using the traditional fixed threshold method for high flow spell detection and a variable threshold for low flow spell detection, the use of a mixed threshold approach for both spells, HFS and LFS, allow us to account for seasonal variability, while still capturing extremes.
- The integration of baseflow estimation techniques, for both HFS and LFS, can be useful as an indicator to determine catchment recovery, pooling successive flood peaks into a single longer duration spells.
- The case study analysis showed a higher predominance of short duration HFS across France, with longer duration HFS occurring primarily in northern France.
- The analysis of transitions between spells demonstrated that consecutive occurrences of the same spell type are most common, with consecutive HFS being more prevalent.
- The regional analysis with the aggregation of results within flood forecasting centers highlighted significant spatial variability in transition characteristics, mainly for transitions from LFS to HFS, with the Mediterranean region showing the shortest transition durations.

The approach developed to identify spatiotemporal patterns of high and low flow spells can be potentially useful to the new generation of multi-hazard early warning systems and to support first responders in flood disaster and drought management (Hammond et al., 2025). Under this perspective, future studies could enhance the approach by fostering validation against impact databases. In our study, validation was limited to cross-checking detected spells against some historic and well documented events. Since impact databases have been increasingly developed, their use to validate compound events could shed light on the amplified socio-economic impacts of short-term transitions, and the appropriate way to define them. Such validation is essential to address the limited understanding of what makes a transition impactful, as current threshold-based methodologies may overlook events that cause significant societal impacts (Anderson et al., 2025). This is relevant given that drought and floods occurring in close succession are associated with amplified socio-economic impacts (Deng et al., 2025), often leading to financial losses and affected populations up to eight times higher than isolated events (Worou and Messori, 2025).

https://doi.org/10.5194/egusphere-2025-6333
Preprint. Discussion started: 7 January 2026

We tested three different baseflow separation methods in our approach, which allowed us to assess differences in the total number of detected spells, and consequently, in spell duration. Other automated baseflow separation techniques could also be tested, such as the Chapman-Maxwell method (Chapman and Maxwell, 1996), the Eckhardt method (Eckhardt, 2005), the delayed-flow separation (Stoelzle et al., 2020), and the AutoVL approach (Lyne, 2025), although we do not think that this would modify our conclusions.

Another important methodological aspect in our approach is the selection of thresholds. This selection can influence the detection of the number of spells and the number of transitions between spells. This threshold sensitivity was also observed by Götte and Brunner (2024), who noted that the number of drought-to-flood transitions decreases both with an increase in the flood threshold and a decrease in the drought threshold. Systematic analyses of different threshold sensitivities could provide insights into the importance of threshold selection in determining not only the characteristics of individual spells but also the frequency and transition types.

Additionally, we found that while most transitions occur between short duration or between short and medium duration spells, the frequency of transitions involving long duration spells or rapid transitions are impacted by threshold selection, resulting in a small sample size, especially for the more severe threshold, that limits the robustness of statistical inference for these events. Complementary approaches, such as those applying surrogate time series by pooling a single model large ensemble (Bevacqua et al., 2023) or seasonal re-forecasts (Klehmet et al., 2024), could enhance the capacity to analyze these less frequent transitions. Moreover, exploring relationships between spell characteristics and catchment attributes or atmospheric patterns would provide deeper insights into the drivers of hydrological spells transitions.

Code availability

The source code utilized to generate the methodology, figures and results presented in this paper may be made available on request from the corresponding author.

Data availability

The CAMELS-FR dataset is publicly available from Delaigue et al. (2024). The boundaries of the 17 flood forecasting centers (SPC) is publicly available from SC Vigicrues (2024). The data and results necessary to replicate the results of this study is publicly available from Guimarães et al. (2025).

Author contribution

GMG: conceptualization, methodology, formal analysis, software, visualization, and writing, MHR: conceptualization, methodology, funding acquisition, supervision, and writing (review and editing), IP: conceptualization, methodology, supervision, and writing (review and editing).

Competing interests

The authors declare that they have no conflict of interest.

Acknowledgements

The authors are grateful to Olivier Delaigue for his assistance with R programming, and Charles Perrin, Vazken Andréassian, and Gustavo Gabbardo for their suggestions.

https://doi.org/10.5194/egusphere-2025-6333
Preprint. Discussion started: 7 January 2026

Financial support

This study was funded by the EU Horizon Europe project MedEWSa (Mediterranean and pan-European forecast and Early Warning System against natural hazards) under Grant Agreement 101121192.

References

Amigues, J.-P., Debaeke, P. P., Itier, B. B., Lemaire, G. G., Seguin, B., Tardieu, F. F., Thomas, A., Uesc, E. S. C., and Pêche, M. de L. E. de L.: Sécheresse et agriculture. Réduire la vulnérabilité de l'agriculture à un risque accru de manque d'eau. Expertise scientifique collective. Synthèse du rapport, INRA, https://doi.org/10.15454/6qrk-4w89, 2006.

Anderson, B. J., Muñoz-Castro, E., Tallaksen, L. M., Matano, A., Götte, J., Armitage, R., Magee, E., and Brunner, M. I.: What is a drought-to-flood transition? Pitfalls and recommendations for defining consecutive hydrological extreme events, Hydrology and Earth System Sciences, 29, 6069–6092, https://doi.org/10.5194/hess-29-6069-2025, 2025.

AON: Weather, Climate and Catastrophe Insight, https://www.aon.com/getmedia/f34ec133-3175-406c-9e0b-25cea768c5cf/20230125-weather-climate-catastrophe-insight.pdf (last access: 21 August 2023), 2023.

Bagheri-Gavkosh, M. and Hosseini, S. M.: Flood Seasonality Analysis in Iran: A Circular Statistics Approach, Journal of Hydrologic Engineering, 28, 04022039, https://doi.org/10.1061/JHYEFF.HEENG-5786, 2023.

Barendrecht, M. H., Matanó, A., Mendoza, H., Weesie, R., Rohse, M., Koehler, J., de Ruiter, M., Garcia, M., Mazzoleni, M., Aerts, J. C. J. H., Ward, P. J., Di Baldassarre, G., Day, R., and Van Loon, A. F.: Exploring drought-to-flood interactions and dynamics: A global case review, WIREs Water, 11, e1726, https://doi.org/10.1002/wat2.1726, 2024.

Barraqué, B., Chery, L., Margat, J., de Marsily, G., and Rieu, T.: Country report for France, in: Groundwater in the Southern Member States of the European Union: an assessment of current knowledge and future prospects, EASAC policy report, 12, edited by: European Academies Science Advisory Council and Deutsche Akademie der Naturforscher Leopoldina, EASAC Secretariat, Deutsche Akademie der Naturforscher Leopoldina, Halle (Saale), p. 45, ISBN 978-3-8047-2827-1, https://easac.eu/fileadmin/PDF_s/reports_statements/France_Groundwater_country_report.pdf (last access: 24 March 2025), 2010.

Berghuijs, W. R. and Slater, L. J.: Groundwater shapes North American river floods, Environ. Res. Lett., 18, 034043, https://doi.org/10.1088/1748-9326/acbecc, 2023.

Bevacqua, E., Suarez-Gutierrez, L., Jézéquel, A., Lehner, F., Vrac, M., Yiou, P., and Zscheischler, J.: Advancing research on compound weather and climate events via large ensemble model simulations, Nat Commun, 14, 2145, https://doi.org/10.1038/s41467-023-37847-5, 2023.

Brett, L., White, C. J., Domeisen, D. I. V., van den Hurk, B., Ward, P., and Zscheischler, J.: Review article: The growth in compound weather and climate event research in the decade since SREX, Natural Hazards and Earth System Sciences, 25, 2591–2611, https://doi.org/10.5194/nhess-25-2591-2025, 2025.

Brunner, M. I. and Chartier-Rescan, C.: Drought Spatial Extent and Dependence Increase During Drought Propagation From the Atmosphere to the Hydrosphere, Geophysical Research Letters, 51, e2023GL107918, https://doi.org/10.1029/2023GL107918, 2024.

Brunner, M. I., Gilleland, E., Wood, A., Swain, D. L., and Clark, M.: Spatial Dependence of Floods Shaped by Spatiotemporal Variations in Meteorological and Land-Surface Processes, Geophysical Research Letters, 47, e2020GL088000, https://doi.org/10.1029/2020GL088000, 2020.

Brunner, M. I., Slater, L., Tallaksen, L. M., and Clark, M.: Challenges in modeling and predicting floods and droughts: A review, WIREs Water, 8, e1520, https://doi.org/10.1002/wat2.1520, 2021.

Brunner, M. I., Van Loon, A. F., and Stahl, K.: Moderate and Severe Hydrological Droughts in Europe Differ in Their Hydrometeorological Drivers, Water Resources Research, 58, e2022WR032871, https://doi.org/10.1029/2022WR032871, 2022.

Brunner, M. I., Anderson, B., and Muñoz-Castro, E.: Meteorological and hydrological dry-to-wet transition events are only weakly related over European catchments, Environ. Res. Lett., 20, 084013, https://doi.org/10.1088/1748-9326/ade72c, 2025.

https://doi.org/10.5194/egusphere-2025-6333
Preprint. Discussion started: 7 January 2026

Caillouet, L., Vidal, J.-P., Sauquet, E., Devers, A., and Graff, B.: Ensemble reconstruction of spatio-temporal extreme low-flow events in France since 1871, Hydrology and Earth System Sciences, 21, 2923–2951, https://doi.org/10.5194/hess-21-2923-2017, 2017.

CCR: Sécheresse de 1996 en France, Caisse Centrale de Réassurance (CCR), Paris, France, https://www.ccr.fr/details-evenements/?event_id=001612 (last access: 29 January 2025), 2018a.

CCR: Sécheresse de 1997 en France, Caisse Centrale de Réassurance (CCR), Paris, France, https://www.ccr.fr/details-evenements/?event_id=001613 (last access: 29 January 2025), 2018b.

CCR: Inondations de la Somme en 2001, Caisse Centrale de Réassurance (CCR), Paris, France, https://www.ccr.fr/details-evenements/?event_id=001335 (last access: 14 October 2024), 2021.

CCR: Les Catastrophes Naturelles en France - Bilan 1982-2023, Caisse Centrale de Réassurance (CCR), Paris, France, https://www.ccr.fr/wp-content/uploads/2025/06/20240605_BILAN_CAT_NAT_DIGITAL_05.06.2024_compressed-1.pdf (last access: 27 June 2024), 2024.

Chapman, T. and Maxwell, A.: Baseflow Separation - Comparison of Numerical Methods with Tracer Experiments, Hydrology and Water Resources Symposium 1996: Water and the Environment; Preprints of Papers, Barton, ACT, https://search.informit.org/doi/epdf/10.3316/informit.360361071346753, 1996.

Chen, H. and Wang, S.: Accelerated Transition Between Dry and Wet Periods in a Warming Climate, Geophysical Research Letters, 49, e2022GL099766, https://doi.org/10.1029/2022GL099766, 2022.

Chen, L. and Ford, T. W.: Future changes in the transitions of monthly-to-seasonal precipitation extremes over the Midwest in Coupled Model Intercomparison Project Phase 6 models, International Journal of Climatology, 43, 255–274, https://doi.org/10.1002/joc.7756, 2023.

Collins, S. L., Christelis, V., Jackson, C. R., Mansour, M. M., Macdonald, D. M. J., and Barkwith, A. K. A. P.: Towards integrated flood inundation modelling in groundwater-dominated catchments, Journal of Hydrology, 591, 125755, https://doi.org/10.1016/j.jhydrol.2020.125755, 2020.

Davison, A. C. and Hinkley, D. V.: Bootstrap Methods and their Application, Cambridge Series in Statistical and Probabilistic Mathematics, Cambridge University Press, Cambridge, https://doi.org/10.1017/CBO9780511802843, 1997.

De Luca, P., Messori, G., Wilby, R. L., Mazzoleni, M., and Di Baldassarre, G.: Concurrent wet and dry hydrological extremes at the global scale, Earth System Dynamics, 11, 251–266, https://doi.org/10.5194/esd-11-251-2020, 2020.

De Ruiter, M. C., Couasnon, A., Van Den Homberg, M. J. C., Daniell, J. E., Gill, J. C., and Ward, P. J.: Why We Can No Longer Ignore Consecutive Disasters, Earth's Future, 8, e2019EF001425, https://doi.org/10.1029/2019EF001425, 2020.

Delaigue, O., Guimarães, G. M., Brigode, P., Génot, B., Perrin, C., and Andréassian, V.: CAMELS-FR dataset, version 1, Recherche Data Gouv [data set], https://doi.org/10.57745/WH7FJR, 2024.

Delaigue, O., Guimarães, G. M., Brigode, P., Génot, B., Perrin, C., Soubeyroux, J.-M., Janet, B., Addor, N., and Andréassian, V.: CAMELS-FR dataset: a large-sample hydroclimatic dataset for France to explore hydrological diversity and support model benchmarking, Earth System Science Data, 17, 1461–1479, https://doi.org/10.5194/essd-17-1461-2025, 2025.

Delforge, D., Wathelet, V., Below, R., Sofia, C. L., Tonnelier, M., van Loenhout, J. A. F., and Speybroeck, N.: EM-DAT: the Emergency Events Database, International Journal of Disaster Risk Reduction, 105509, https://doi.org/10.1016/j.ijdrr.2025.105509, 2025.

Deng, S., Guntu, R. K., Khosh Bin Ghomash, S., Zhao, D., and Kreibich, H.: Economic consequences of cascading drought-flood events: evidence from central Europe, Environ. Res. Lett., 20, 114028, https://doi.org/10.1088/1748-9326/ae0f43, 2025.

Diederen, D., Liu, Y., Gouldby, B., Diermanse, F., and Vorogushyn, S.: Stochastic generation of spatially coherent river discharge peaks for continental event-based flood risk assessment, Natural Hazards and Earth System Sciences, 19, 1041–1053, https://doi.org/10.5194/nhess-19-1041-2019, 2019.

DIREN Midi-Pyrénées: Bilan Hydrologique du Bassin Adour-Garonne au 31/10/2003, Direction Régionale de l'Environnement (DIREN) Midi-Pyrénées, Service de Bassin Adour-Garonne, https://www.occitanie.developpement-durable.gouv.fr/IMG/pdf/BILAN_DE_1_ETIAGE_2003_c1e7e9c5c.pdf (last access: 6 November 2025), 2003.

https://doi.org/10.5194/egusphere-2025-6333
Preprint. Discussion started: 7 January 2026

Duncan, H. P.: Baseflow separation – A practical approach, Journal of Hydrology, 575, 308–313, https://doi.org/10.1016/j.jhydrol.2019.05.040, 2019.

Eckhardt, K.: How to construct recursive digital filters for baseflow separation, Hydrological Processes, 19, 507–515, https://doi.org/10.1002/hyp.5675, 2005.

Fang, B. and Lu, M.: Asia Faces a Growing Threat From Intraseasonal Compound Weather Whiplash, Earth's Future, 11, e2022EF003111, https://doi.org/10.1029/2022EF003111, 2023.

Fang, B., Bevacqua, E., Rakovec, O., and Zscheischler, J.: An increase in the spatial extent of European floods over the last 70 years, Hydrology and Earth System Sciences, 28, 3755–3775, https://doi.org/10.5194/hess-28-3755-2024, 2024.

Fischer, S. and Schumann, A. H.: Dominant flood types in Europe and their role in flood statistics, Hydrological Sciences Journal, 0, 1–17, https://doi.org/10.1080/02626667.2025.2450369, 2025.

Fischer, S., Pahlow, M., and Singh, S. K.: Impact of catchment and climate attributes on flood generating processes and their effect on flood statistics, Journal of Hydrology, 646, 132361, https://doi.org/10.1016/j.jhydrol.2024.132361, 2025.

Fleig, A. K., Tallaksen, L. M., Hisdal, H., and Demuth, S.: A global evaluation of streamflow drought characteristics, Hydrology and Earth System Sciences, 10, 535–552, https://doi.org/10.5194/hess-10-535-2006, 2006.

García-Portugués, E., Verdebout, T., Fernández-de-Marcos, A., and Navarro, P.: sphunif: Uniformity Tests on the Circle, Sphere, and Hypersphere, R package, version 1.4.0, CRAN [code], https://doi.org/10.32614/CRAN.package.sphunif, 2024.

Godet, J., Payrastre, O., Ding, Q., Demargne, J., Gaume, E., Nicolle, P., Belleudy, A., and Javelle, P.: Evaluating the French Flash Flood Warning System Using Hydrological and Impact Data in Southeastern France, Journal of Flood Risk Management, 18, e70053, https://doi.org/10.1111/jfr3.70053, 2025.

Götte, J. and Brunner, M. I.: Hydrological Drought-To-Flood Transitions Across Different Hydroclimates in the United States, Water Resources Research, 60, e2023WR036504, https://doi.org/10.1029/2023WR036504, 2024.

Guimarães, G. M., Ramos, M.-H., and Pechlivanidis, I.: Characteristics of low and high flow spells and their temporal transitions in France, version 1.0, Recherche Data Gouv [data set], https://doi.org/10.57745/TNKVAY, 2025.

Habets, F., Gascoin, S., Korkmaz, S., Thiéry, D., Zribi, M., Amraoui, N., Carli, M., Ducharne, A., Leblois, E., Ledoux, E., Martin, E., Noilhan, J., Ottlé, C., and Viennot, P.: Multi-model comparison of a major flood in the groundwater-fed basin of the Somme River (France), Hydrology and Earth System Sciences, 14, 99–117, https://doi.org/10.5194/hess-14-99-2010, 2010.

Hall, J. and Blöschl, G.: Spatial patterns and characteristics of flood seasonality in Europe, Hydrology and Earth System Sciences, 22, 3883–3901, https://doi.org/10.5194/hess-22-3883-2018, 2018.

Hammond, J., Anderson, B., Simeone, C., Brunner, M., Muñoz-Castro, E., Archfield, S., Magee, E., and Armitage, R.: Hydrological Whiplash: Highlighting the Need for Better Understanding and Quantification of Sub-Seasonal Hydrological Extreme Transitions, Hydrological Processes, 39, e70113, https://doi.org/10.1002/hyp.70113, 2025.

Hariharan Sudha, S., Ragno, E., Morales-Nápoles, O., and Kok, M.: Investigating meteorological wet and dry transitions in the Dutch Meuse River basin, Front. Water, 6, https://doi.org/10.3389/frwa.2024.1394563, 2024.

He, X. and Sheffield, J.: Lagged Compound Occurrence of Droughts and Pluvials Globally Over the Past Seven Decades, Geophysical Research Letters, 47, e2020GL087924, https://doi.org/10.1029/2020GL087924, 2020.

Hellwig, J. and Stahl, K.: An assessment of trends and potential future changes in groundwater-baseflow drought based on catchment response times, Hydrology and Earth System Sciences, 22, 6209–6224, https://doi.org/10.5194/hess-22-6209-2018, 2018.

Hellwig, J., Stoelzle, M., and Stahl, K.: Groundwater and baseflow drought responses to synthetic recharge stress tests, Hydrology and Earth System Sciences, 25, 1053–1068, https://doi.org/10.5194/hess-25-1053-2021, 2021.

Heudorfer, B. and Stahl, K.: Comparison of different threshold level methods for drought propagation analysis in Germany, Hydrology Research, 48, 1311–1326, https://doi.org/10.2166/nh.2016.258, 2017.

Hillier, J. K., Matthews, T., Wilby, R. L., and Murphy, C.: Multi-hazard dependencies can increase or decrease risk, Nat. Clim. Chang., 10, 595–598, https://doi.org/10.1038/s41558-020-0832-y, 2020.

https://doi.org/10.5194/egusphere-2025-6333
Preprint. Discussion started: 7 January 2026

Hisdal, H., Tallaksen, L. M., Gauster, T., Bloomfield, J. P., Parry, S., Prudhomme, C., and Wanders, N.: Hydrological drought characteristics, in: Hydrological Drought (Second Edition), edited by: Tallaksen, L. M. and van Lanen, H. A. J., Elsevier, p. 157–231, https://doi.org/10.1016/B978-0-12-819082-1.00006-0, 2024.

van den Hurk, B. J. J. M., White, C. J., Ramos, A. M., Ward, P. J., Martius, O., Olbert, I., Roscoe, K., Goulart, H. M. D., and Zscheischler, J.: Consideration of compound drivers and impacts in the disaster risk reduction cycle, iScience, 26, 106030, https://doi.org/10.1016/j.isci.2023.106030, 2023.

Jones, R. L., Kharb, A., and Tubeuf, S.: The untold story of missing data in disaster research: a systematic review of the empirical literature utilising the Emergency Events Database (EM-DAT), Environ. Res. Lett., 18, 103006, https://doi.org/10.1088/1748-9326/acfd42, 2023.

Klehmet, K., Berg, P., Bozhinova, D., Crochemore, L., Du, Y., Pechlivanidis, I., Photiadou, C., and Yang, W.: Robustness of hydrometeorological extremes in surrogated seasonal forecasts, Intl Journal of Climatology, 44, 1725–1738, https://doi.org/10.1002/joc.8407, 2024.

Kratzert, F., Nearing, G., Addor, N., Erickson, T., Gauch, M., Gilon, O., Gudmundsson, L., Hassidim, A., Klotz, D., Nevo, S., Shalev, G., and Matias, Y.: Caravan - A global community dataset for large-sample hydrology, Sci Data, 10, 61, https://doi.org/10.1038/s41597-023-01975-w, 2023.

Kreibich, H. and Thieken, A. H.: Assessment of damage caused by high groundwater inundation, Water Resources Research, 44, W09409, https://doi.org/10.1029/2007WR006621, 2008.

Laaha, G. and Koffler, D.: lfstat: Calculation of Low Flow Statistics for Daily Stream Flow Data, R package, version 0.9.12, CRAN [code], https://doi.org/10.32614/CRAN.package.lfstat, 2022.

Ladson, A. R., Brown, R., Neal, B., and Nathan, R.: A Standard Approach to Baseflow Separation Using The Lyne and Hollick Filter, Australasian Journal of Water Resources, 17, 25–34, https://doi.org/10.7158/13241583.2013.11465417, 2013.

Ladson, T.: BaseflowSeparation_LyneHollick, GitHub [code], https://github.com/TonyLadson/BaseflowSeparation_LyneHollick (last access: 4 December 2025), 2013.

Landler, L., Ruxton, G. D., and Malkemper, E. P.: The Hermans–Rasson test as a powerful alternative to the Rayleigh test for circular statistics in biology, BMC Ecol, 19, 30, https://doi.org/10.1186/s12898-019-0246-8, 2019.

de Lavenne, A., Andréassian, V., Crochemore, L., Lindström, G., and Arheimer, B.: Quantifying multi-year hydrological memory with Catchment Forgetting Curves, Hydrology and Earth System Sciences, 26, 2715–2732, https://doi.org/10.5194/hess-26-2715-2022, 2022.

Lehner, B.: HydroRIVERS - Global river network delineation derived from HydroSHEDS data at 15 arc-second resolution, version 1.0, HydroSHEDS [data set], https://www.hydrosheds.org/products/hydrorivers (last access: 10 December 2025), 2019.

Lehner, B. and Grill, G.: Global river hydrography and network routing: baseline data and new approaches to study the world's large river systems, Hydrological Processes, 27, 2171–2186, https://doi.org/10.1002/hyp.9740, 2013.

Leonard, M., Westra, S., Phatak, A., Lambert, M., van den Hurk, B., McInnes, K., Risbey, J., Schuster, S., Jakob, D., and Stafford-Smith, M.: A compound event framework for understanding extreme impacts, WIREs Climate Change, 5, 113–128, https://doi.org/10.1002/wcc.252, 2014.

Ley, C. and Verdebout, T.: Modern directional statistics, 1st ed., Chapman & Hall CRC, New York, 190 pp., https://doi.org/10.1201/9781315119472, 2017.

Li, X., Zhang, Q., Zhang, D., and Ye, X.: Investigation of the drought–flood abrupt alternation of streamflow in Poyang Lake catchment during the last 50 years, Hydrology Research, 48, 1402–1417, https://doi.org/10.2166/nh.2016.266, 2016.

Lindersson, S., Brandimarte, L., Mård, J., and Di Baldassarre, G.: A review of freely accessible global datasets for the study of floods, droughts and their interactions with human societies, WIREs Water, 7, e1424, https://doi.org/10.1002/wat2.1424, 2020.

Longobardi, A. and Van Loon, A. F.: Assessing baseflow index vulnerability to variation in dry spell length for a range of catchment and climate properties, Hydrological Processes, 32, 2496–2509, https://doi.org/10.1002/hyp.13147, 2018.

https://doi.org/10.5194/egusphere-2025-6333
Preprint. Discussion started: 7 January 2026

Lyne, V.: AutoVL: Automated streamflow separation for changing catchments and climate impact analysis, Journal of Hydrology X, 26, 100195, https://doi.org/10.1016/j.hydroa.2024.100195, 2025.

Lyne, V. and Hollick, M.: Stochastic timevariable rainfall-runoff modelling, in: Hydrology and Water Resources Symposium: symposium papers, National conference publication, 79/10, Hydrology and Water Resources Symposium, Perth, 10-12 September 1979, 89–92, ISBN 0-85825-114-0, 1979.

Mardia, K. V. and Jupp, P. E.: Directional statistics, Wiley series in probability and statistics, J. Wiley, Chichester ; New York, 429 pp., ISBN 978-0-471-95333-3, 2000.

Matanó, A., Berghuijs, W. R., Mazzoleni, M., de Ruiter, M. C., Ward, P. J., and Van Loon, A. F.: Compound and consecutive drought-flood events at a global scale, Environ. Res. Lett., 19, 064048, https://doi.org/10.1088/1748-9326/ad4b46, 2024.

Mei, Y. and Anagnostou, E. N.: A hydrograph separation method based on information from rainfall and runoff records, Journal of Hydrology, 523, 636–649, https://doi.org/10.1016/j.jhydrol.2015.01.083, 2015.

NOAA: Global Self-consistent, Hierarchical, High-resolution Geography Database (GSHHG), version 2.3.7, National Oceanic and Atmospheric Administration (NOAA) [data set], https://www.ngdc.noaa.gov/mgg/shorelines/shorelines.html (last access: 10 December 2025), 2017.

Pan, X., Rahman, A., Haddad, K., and Ouarda, T. B. M. J.: Peaks-over-threshold model in flood frequency analysis: a scoping review, Stoch Environ Res Risk Assess, 36, 2419–2435, https://doi.org/10.1007/s00477-022-02174-6, 2022.

Parry, S., Hannaford, J., Lloyd-Hughes, B., and Prudhomme, C.: Multi-year droughts in Europe: analysis of development and causes, Hydrology Research, 43, 689–706, https://doi.org/10.2166/nh.2012.024, 2012.

Pelletier, A. and Andréassian, V.: Hydrograph separation: an impartial parametrisation for an imperfect method, Hydrology and Earth System Sciences, 24, 1171–1187, https://doi.org/10.5194/hess-24-1171-2020, 2020.

Pelletier, A., Andréassian, V., and Delaigue, O.: baseflow: Computes Hydrograph Separation, R package, version 1.0, INRAE [code], https://doi.org/10.15454/Z9IK5N, 2020.

Pennequin, D.: Toward a water cycle approach for flood risk assessment …, AQUAmundi, 7–12, https://doi.org/10.4409/Am-003-10-0002, 2010.

Piggott, A. R., Moin, S., and Southam, C.: A revised approach to the UKIH method for the calculation of baseflow / Une approche améliorée de la méthode de l'UKIH pour le calcul de l'écoulement de base, Hydrological Sciences Journal, 50, 920, https://doi.org/10.1623/hysj.2005.50.5.911, 2005.

Qing, Y., Wang, S., Yang, Z.-L., and Gentine, P.: Soil moisture−atmosphere feedbacks have triggered the shifts from drought to pluvial conditions since 1980, Commun Earth Environ, 4, 1–10, https://doi.org/10.1038/s43247-023-00922-2, 2023.

Quesada-Montano, B., Di Baldassarre, G., Rangecroft, S., and Van Loon, A. F.: Hydrological change: Towards a consistent approach to assess changes on both floods and droughts, Advances in Water Resources, 111, 31–35, https://doi.org/10.1016/j.advwatres.2017.10.038, 2018.

RahimiMovaghar, M., Fereshtehpour, M., and Najafi, M. R.: Spatiotemporal pattern of successive hydro-hazards and the influence of low-frequency variability modes over Canada, Journal of Hydrology, 634, 131057, https://doi.org/10.1016/j.jhydrol.2024.131057, 2024.

Rashid, M. M. and Wahl, T.: Hydrologic risk from consecutive dry and wet extremes at the global scale, Environ. Res. Commun., 4, 071001, https://doi.org/10.1088/2515-7620/ac77de, 2022.

Sarremejane, R., Messager, M. L., and Datry, T.: Drought in intermittent river and ephemeral stream networks, Ecohydrology, 15, e2390, https://doi.org/10.1002/eco.2390, 2022.

SC Vigicrues: Territoires de Compétence Crues (TCC) - Métropole, Service Central Vigicrues (SC Vigicrues) [data set], https://www.sandre.eaufrance.fr/atlas/srv/fre/catalog.search#/metadata/b0850826-cdf9-4666-87a6-f47e6d3b0191 (last access: 8 December 2025), 2024.

Seneviratne, S. I., Zhang, X., Adnan, M., Badi, W., Dereczynski, C., Di Luca, A., Ghosh, S., Iskandar, I., Kossin, J., Lewis, S., Otto, F., Pinto, I., Satoh, M., Vicente-Serrano, S. M., Wehner, M., and Zhou, B.: Weather and climate extreme events in a changing climate, in: Climate Change 2021: The Physical Science Basis. Contribution of Working Group I to the Sixth Assessment Report of the Intergovernmental Panel on Climate Change, edited by: Masson-Delmotte, V., Zhai, P., Pirani, A.,

https://doi.org/10.5194/egusphere-2025-6333
Preprint. Discussion started: 7 January 2026

Connors, S. L., Péan, C., Berger, S., Caud, N., Chen, Y., Goldfarb, L., Gomis, M. I., Huang, M., Leitzell, K., Lonnoy, E., Matthews, J. B. R., Maycock, T. K., Waterfield, T., Yelekçi, Ö., Yu, R., and Zhou, B., Cambridge University Press, Cambridge, United Kingdom and New York, NY, USA, p. 1513–1766, https://doi.org/10.1017/9781009157896, 2021.

Stoelzle, M., Schuetz, T., Weiler, M., Stahl, K., and Tallaksen, L. M.: Beyond binary baseflow separation: a delayed-flow index for multiple streamflow contributions, Hydrology and Earth System Sciences, 24, 849–867, https://doi.org/10.5194/hess-24-849-2020, 2020.

Tarasova, L., Basso, S., Zink, M., and Merz, R.: Exploring Controls on Rainfall-Runoff Events: 1. Time Series-Based Event Separation and Temporal Dynamics of Event Runoff Response in Germany, Water Resources Research, 54, 7711–7732, https://doi.org/10.1029/2018WR022587, 2018.

Tramblay, Y., Arnaud, P., Artigue, G., Lang, M., Paquet, E., Neppel, L., and Sauquet, E.: Changes in Mediterranean flood processes and seasonality, Hydrology and Earth System Sciences, 27, 2973–2987, https://doi.org/10.5194/hess-27-2973-2023, 2023.

UKIH: Low Flow Studies, Institute of Hydrology, Wallingford, UK, https://nora.nerc.ac.uk/id/eprint/9093 (last access: 21 January 2025), 1980.

Van Loon, A. F.: Hydrological drought explained, WIREs Water, 2, 359–392, https://doi.org/10.1002/wat2.1085, 2015.

Van Loon, A. F. and Laaha, G.: Hydrological drought severity explained by climate and catchment characteristics, Journal of Hydrology, 526, 3–14, https://doi.org/10.1016/j.jhydrol.2014.10.059, 2015.

Vigoureux, S., Brigode, P., Ramos, M.-H., Poggio, J., Dreyfus, R., Moreau, E., Laroche, C., and Tric, E.: Spatio-temporal characteristics of heavy precipitation events observed over the last decade on the eastern French Mediterranean coastal area, Journal of Hydrology: Regional Studies, 56, 101988, https://doi.org/10.1016/j.ejrh.2024.101988, 2024.

Ward, P. J., de Ruiter, M. C., Mård, J., Schröter, K., Van Loon, A., Veldkamp, T., von Uexkull, N., Wanders, N., AghaKouchak, A., Arnbjerg-Nielsen, K., Capewell, L., Carmen Llasat, M., Day, R., Dewals, B., Di Baldassarre, G., Huning, L. S., Kreibich, H., Mazzoleni, M., Savelli, E., Teutschbein, C., van den Berg, H., van der Heijden, A., Vincken, J. M. R., Waterloo, M. J., and Wens, M.: The need to integrate flood and drought disaster risk reduction strategies, Water Security, 11, 100070, https://doi.org/10.1016/j.wasec.2020.100070, 2020.

Ward, P. J., Daniell, J., Duncan, M., Dunne, A., Hananel, C., Hochrainer-Stigler, S., Tijssen, A., Torresan, S., Ciurean, R., Gill, J. C., Sillmann, J., Couasnon, A., Koks, E., Padrón-Fumero, N., Tatman, S., Tronstad Lund, M., Adesiyun, A., Aerts, J. C. J. H., Alabaster, A., Bulder, B., Campillo Torres, C., Critto, A., Hernández-Martín, R., Machado, M., Mysiak, J., Orth, R., Palomino Antolín, I., Petrescu, E.-C., Reichstein, M., Tiggeloven, T., Van Loon, A. F., Vuong Pham, H., and de Ruiter, M. C.: Invited perspectives: A research agenda towards disaster risk management pathways in multi-(hazard-)risk assessment, Natural Hazards and Earth System Sciences, 22, 1487–1497, https://doi.org/10.5194/nhess-22-1487-2022, 2022.

Wessel, P. and Smith, W. H. F.: A global, self-consistent, hierarchical, high-resolution shoreline database, J. Geophys. Res.-Sol. Ea., 101, 8741–8743, https://doi.org/10.1029/96JB00104, 1996.

WMO: WMO Atlas of Mortality and Economic Losses from Weather, Climate and Water Extremes (1970–2019), WMO, 1267, World Meteorological Organization (WMO), Geneva, 90 pp., ISBN 978-92-63-11267-5, 2021.

Worou, K. and Messori, G.: Compounding droughts and floods amplify socio-economic impacts, Environ. Res. Lett., 20, 104024, https://doi.org/10.1088/1748-9326/adfe82, 2025.

Zscheischler, J., Martius, O., Westra, S., Bevacqua, E., Raymond, C., Horton, R. M., van den Hurk, B., AghaKouchak, A., Jézéquel, A., Mahecha, M. D., Maraun, D., Ramos, A. M., Ridder, N. N., Thiery, W., and Vignotto, E.: A typology of compound weather and climate events, Nat Rev Earth Environ, 1, 333–347, https://doi.org/10.1038/s43017-020-0060-z, 2020.